creative commons
COMMONS DEED

저작자표시-비영리-변경금지 2.0 대한민국

이용자는 아래의 조건을 따르는 경우에 한하여 자유롭게

- 이 저작물을 복제, 배포, 전송, 전시, 공연 및 방송할 수 있습니다.

다음과 같은 조건을 따라야 합니다:

저작자표시. 귀하는 원저작자를 표시하여야 합니다.

비영리. 귀하는 이 저작물을 영리 목적으로 이용할 수 없습니다.

변경금지. 귀하는 이 저작물을 개작, 변형 또는 가공할 수 없습니다.

- 귀하는, 이 저작물의 재이용이나 배포의 경우, 이 저작물에 적용된 이용허락조건을 명확하게 나타내어야 합니다.
- 저작권자로부터 별도의 허가를 받으면 이러한 조건들은 적용되지 않습니다.

저작권법에 따른 이용자의 권리는 위의 내용에 의하여 영향을 받지 않습니다.

이것은 이용허락규약(Legal Code)을 이해하기 쉽게 요약한 것입니다.

Disclaimer

dCollection

ULSAN NATIONAL INSTITUTE OF SCIENCE AND TECHNOLOGY

Master's Thesis

Effects of Sizing Materials on the Properties of Carbon Fiber-Reinforced Polyamide 6 Composites Manufactured through Thermoplastic Resin Transfer Molding

Sang-Hyup Cha

Department of Mechanical Engineering

Graduate School of UNIST

2019

ULSAN NATIONAL INSTITUTE OF
SCIENCE AND TECHNOLOGY

Effects of Sizing Materials on the Properties of Carbon Fiber-Reinforced Polyamide 6 Composites Manufactured through Thermoplastic Resin Transfer Molding

Sang-Hyup Cha

Department of Mechanical Engineering

Graduate School of UNIST

ULSAN NATIONAL INSTITUTE OF
SCIENCE AND TECHNOLOGY

Effects of Sizing Materials on the Properties of Carbon Fiber-Reinforced Polyamide 6 Composites Manufactured through Thermoplastic Resin Transfer Molding

A thesis
submitted to the Graduate School of UNIST
in partial fulfillment of the
requirements for the degree of
Master of Science

Sang-Hyup Cha

December 11, 2018

Approved by

Advisor

Young-Bin Park

ULSAN NATIONAL INSTITUTE OF
SCIENCE AND TECHNOLOGY

Effects of Sizing Materials on the Properties of Carbon Fiber-Reinforced Polyamide 6 Composites Manufactured through Thermoplastic Resin Transfer Molding

Sang-Hyup Cha

This certifies that the thesis of Sang-Hyup Cha is approved.

December 11, 2018

signature

Advisor: Young-Bin Park

signature

Wooseok Ji

signature

Han Gi Chae

ULSAN NATIONAL INSTITUTE OF SCIENCE AND TECHNOLOGY

Abstract

Carbon fiber reinforced plastics (CFRPs) are a combination of high-strength and stiffness carbon fiber and resin, and the weight of the composite is less than one-half the weight of similar rigid, ultra-high tensile steel plates. However, CFRP is 4.4 times more expensive than ultra-high tensile steel parts, and 30 percent lighter than aluminum but 3.8 times more expensive. Therefore, it is necessary to reduce the costs of CFRPs to broaden the market to the mechanical and aerospace industries. A variety of composite manufacturing processes were developed to minimize the processing time.

Among them, thermoplastic resin transfer molding (T-RTM) using the anionic ring opening polymerization of ε-caprolactam transfers the monomer into the mold with the catalyst and activator, leading to polymerization and crystallization simultaneously. Melt viscosity of ε-caprolactam is 100 times lower than thermoset resins in reaction processing and 160,000 times lower than thermoplastic resins in melting processing. Thus, the T-RTM process has the advantage of fewer limitations in production structure, good resin impregnation, and short production cycle time – in the order of a few minutes.

One of the most important factors affecting the properties of composite materials is the adhesion at the fiber-matrix interfaces. The fiber-matrix adhesion is strongly associated with load transfer efficiency inside the composite, and thus affects the overall mechanical properties of the material. In this study, sizing process was used to enhance the fiber-matrix adhesion**.** Sizing refers to coating the surface of a fiber with a thin polymer, and in a way that has become common, most commercial fibers have already been coated with sizing materials.

A total of seven sizing materials, expected to be highly compatible with A-PA6, were used. Physical and chemical changes of the carbon fiber surface by sizing materials were analyzed by TGA, SEM, XPS, and FT-IR. Also, fiber-bundle pull-out test, short beam test, and X-ray micro CT were conducted to measure the IFSS, short beam strength, and void content of the composite manufactured by T-RTM.

Consequently, the highest improvements in IFSS and short beam strength were 30 and 50% achieved with epoxy (EP) and polyamide (PA) sizings, respectively, due to enhanced fiber-matrix adhesion with A-PA6 resin. The improvement mechanisms of fiber-matrix adhesion by

ULSAN NATIONAL INSTITUTE OF
SCIENCE AND TECHNOLOGY

EP and PA were verified by XPS, surface energy, X-ray micro CT and FT-IR analysis. As a results, EP and PA sizing materials were proven to be the most suitable for T-RTM process.

ULSAN NATIONAL INSTITUTE OF SCIENCE AND TECHNOLOGY

Contents

ULSAN NATIONAL INSTITUTE OF SCIENCE AND TECHNOLOGY

ULSAN NATIONAL INSTITUTE OF SCIENCE AND TECHNOLOGY

List of Figures

ULSAN NATIONAL INSTITUTE OF SCIENCE AND TECHNOLOGY

ULSAN NATIONAL INSTITUTE OF SCIENCE AND TECHNOLOGY

List of Tables

ULSAN NATIONAL INSTITUTE OF SCIENCE AND TECHNOLOGY

1. Introduction

Carbon fiber reinforced plastics (CFRPs) are a combination of high strength and stiffness carbon fiber and polymer matrix resin, and the weight of the composite is less than one-half the weight of similar rigid, ultra-high tensile steel plates. Due to these characteristics, as a lightweight material, composite materials have been used for aerospace, sporting goods, wind power blades, medical devices, electronics, automobiles, etc., and reinforcement of building structures.

In particular, it is estimated to have a 10.6% annual growth rate over the next 10 years due to improved fuel efficiency of automobiles and aircraft, increased demand for high-performance products such as light-weight and x-ray permeability[10]. In addition, in the case of electric vehicles, the weight of the body battery is heavy, making light weight necessary to increase the mileage. As a result, the size of the market is expected to change significantly, along with the increase in the use of CFRP components. Airbus' A350 model used 53 percent of its carbon composite materials as a structural material[11], and BMW's i3, the first mass-produced electric car, was lightened using about 150kg CFRP parts[12].

However, CFRP is 4.4 times more expensive than ultra-high tensile steel parts and 30 percent lighter than aluminum, but 3.8 times more expensive. Therefore, it is necessary to reduce costs to broaden the market to the mechanical and aerospace industries[13]. To overcome this, research is underway on the development of low-cost carbon fiber production and high-speed composite manufacturing process. A variety of composite manufacturing processes were developed to minimize the processing time, while Mitsubishi Rayon developed thermoplastic SMC hybrid molding technology with thermoset or thermoplastic prepreg compression molding, and the HP-RTM process, which is effective in forming complex shape thermoset CFRP parts, reduced the processing time to within three minutes. In addition, T-RTM, a thermoplastic CFRP manufacturing process, has been developed that uses anionic ring opening polymerization of ε-caprolactam to solve the impregnation problem, and Huntsman developed a wet compression molding process that allows parts with complex shapes to be molded in one minute compared to conventional methods[14].

Thermoplastic CFRPs have excellent impact resistance and toughness, can be recycled and hot-welded, and production cost is relatively low, so technology development has been actively

ULSAN NATIONAL INSTITUTE OF SCIENCE AND TECHNOLOGY

carried out. Accordingly, developments of thermoplastic CFRP parts manufactured by LFT, unidirectional (UD) tape, prepreg, T-RTM and over-molding process are increasing. Among them, the T-RTM process using the anionic ring opening polymerization of ε-caprolactam transfers the monomer into the mold with the catalyst and activator at the melt state, the monomer immediately reacts with catalyst and activator, leading polymerization and crystallization simultaneously at below the polymer and crystallization point. Melt viscosity of ε-caprolactam is 100 times lower than thermoset resins of reaction processing and 160,000 times lower than thermoplastic resins of the melting processing[2]. Thus, the T-RTM process has the advantage of few limitations of production structure, well-impregnation of resin and only a few minutes for a production cycle[4].

One of the important properties of the composite materials is the fiber-matrix adhesion. The fiber-matrix adhesion is strongly associated with load transfer efficiency inside the composite, and thus affects the overall mechanical properties of the material[15]. The weakest part of CFRP is the interphase between the fiber and resin because of the inert surface of carbon fiber. For this reason, studies have been conducted to strengthen the fiber-matrix adhesion. There is a method of matrix modification by using nanomaterials such as carbon nanotubes (CNTs)[16-18], nanoclay[19-21], exfoliated graphene nanoplatelets[17, 22] and graphene oxide (GO)[23, 24], or using compatibilizers such as PP-g-MA[25] and SEBS-g-MA[26]. Other typical method is the surface treatment of fibers, including fiber sizing[27-29], acidic modification[30-32], plasma surface modification[4, 33, 34] and whiskerization[5, 6, 35]. However, considering the limitations of nanomaterial dispersion, mass production, environmental issues of acidic solvents, and long processing time, this study was intended to enhance the fiber-matrix adhesion by sizing process**.** Sizing refers to coating the surface of a fiber with a thin polymer, and in a way that has become common, most commercial fibers have already been coated with sizing materials. Sizing material prevents brittle fibers from external damage and provides suitable strand integrity. Then, according to the compatibility of the fiber/sizing/matrix, it increases the fiber-matrix adhesion[15]. In particular, the sizing process is very simple, and can be carried out in mass production when applied to the industry, which is consistent with the development trend of high-speed manufacturing technologies.

When determining sizing materials suitable for composite manufacturing processes, fibers, resins, manufacturing process conditions, and usage of composite materials should be

ULSAN NATIONAL INSTITUTE OF SCIENCE AND TECHNOLOGY

considered. T-RTM, a composite manufacturing process used in this study, uses ε-caprolactam which is a monomer of polyamide 6 (PA6). The monomer reacts with the ion type of catalyst, opens the ring structure, and creates a single chain of PA6. This polymerization process occurs repeatedly, and the polymer PA6 is made, which is called anionic polyamide 6 (A-PA6). Due to the use of catalyst and activator, the process temperature becomes relatively low, but it is very sensitive to moisture and polymerization conditions[1]. During the polymerization process, A-PA6 reacts with the sizing materials, and it has various effects on the polymerization in the interphase region. These chemical reactions affect the fiber-matrix adhesion, which in turn possibly affects the overall mechanical properties of the composite. Currently, research on sizing effects on the reactive thermoplastic manufacturing processes such as T-RTM is insufficient.

Therefore, in this study, the sizing materials suitable for the T-RTM process was investigated. A total of seven sizing materials, expected to be highly compatible with A-PA6, were used to analyze the physical and chemical changes in coated fiber surfaces. Using the T-RTM process, coated carbon fiber reinforced A-PA6 composites were manufactured, and the mechanical properties analysis of composite materials and the chemical reaction analysis of sizing/A-PA6 examined the effects of sizing on the fiber-matrix adhesion.

ULSAN NATIONAL INSTITUTE OF SCIENCE AND TECHNOLOGY

2. Literature Review

2.1 Reactive Processing of Thermoplastic PA6

The reactive processing of PA6 has a lot of advantages on a high impact resistance, recyclable and well-impregnation due to its low melt viscosity. Therefore, it has an attention from research into the manufacturing process of continuous fiber reinforced thermoplastic composite. Only few thermoplastics can be used for the reactive process. Rijswijk *et al*[1, 36-40]. investigated thermoplastics suitable for the reactive process. According to the literature, the PA6 monomer has a very low melt viscosity, and the temperature of the catalyzed reaction occurs around 130-170℃, which is lower than other processes (**Fig. 1**a). Depending on the ratio of catalyst and activator, the final monomer conversion can be over 99.3% within 3-60 minutes. Also, polymerization and crystallization occur together because the process temperature is lower than the melting temperature and the crystallization point of A-PA6, and as a result it can be high crystalline PA6.

Berg *et al.*[2] introduced the process of reactive injection molding (RIM) using anionic ring opening polymerization of ε-caprolactam. In choosing the proper resin for the RIM process, he considered the low melt viscosity, rapid polymerization and crystallization, isothermal low temperature processing and low price. Several parameters and equipment were modified to develop the RIM process (**Fig. 1**b), which was mainly used for thermoset resin, to the characteristics of A-PA6, and the continuous glass fiber reinforced A-PA6 was produced.

Pillay *et al*.[3, 41] introduced the vacuum received transfer molding (VARTM) process, which used reactive processing of PA6 (**Fig. 1**c), and produced continuous carbon fiber reinforced A-PA6 composite. VARTM is a process that mainly uses thermoset resin. The ratio of catalyst and activator, humidity minimizing, injection technology, and temperature control were optimized to achieve low melt viscosity, adequate processing time, and sufficient impregnation and polymerization. When resin was injected at 100℃, the result showed higher fiber volume fraction, crystallinity, and degree of monomer conversion (~98%) than injection case at 150℃.

Kim *et al*.[4, 6] optimized the thermoplastic-resin transfer molding (T-RTM) process using the anionic ring opening polymerization of ε-caprolactam through various studies (**Fig. 1**d). T-RTM process has the advantages including simple equipment and low void percent inside the

ULSAN NATIONAL INSTITUTE OF SCIENCE AND TECHNOLOGY

composite. The ratio of the catalyst and activator, processing temperature, and processing cycle were optimized. Through the studies, the results showed 3.7 and 2.9 wt.% of catalyst and activator ratio, 150℃ processing temperature, 25s of polymerization time, less than 5 minutes of production cycle, and 98% of monomer conversion.

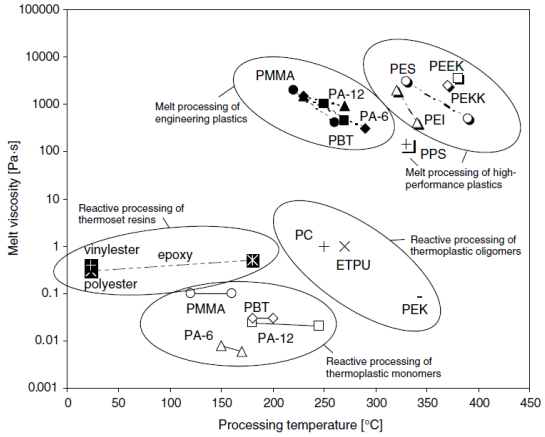

(a)

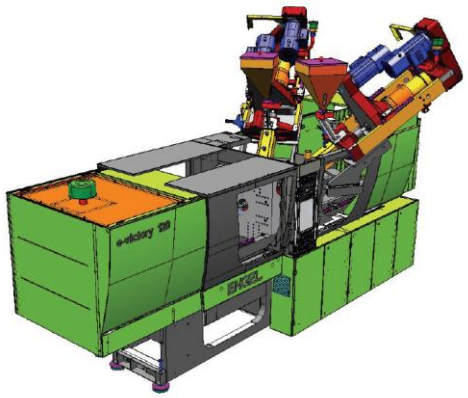

(b)

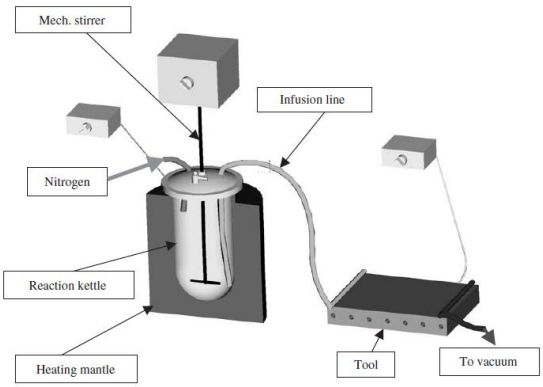

(c)

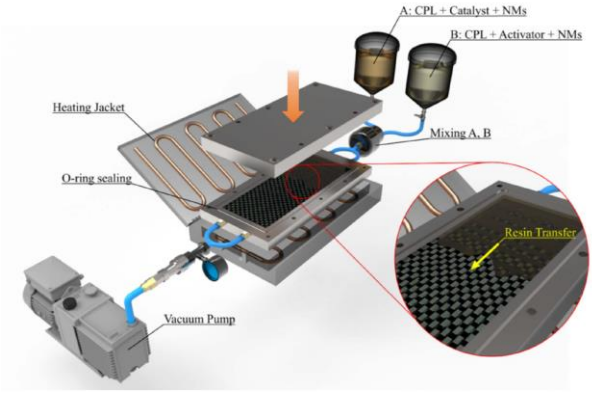

(d)

Figure 1. Various matrix materials and several methods of reactive processing of thermoplastic PA6: (a) Melt viscosities and processing temperatures of various matrix materials for both reactive and melt processing[1], (b) prototype of injection molding machine for reactive injection molding[2], (c) schematic of VARTM[3], (d) Processing schematics of T-RTM[4].

ULSAN NATIONAL INSTITUTE OF SCIENCE AND TECHNOLOGY

2.2 Improvement Method for Fiber-Matrix Adhesion

The mechanical properties of fiber reinforced composite materials are highly correlated with the fiber-matrix adhesion. An increase in the fiber-matrix adhesion improves the load transfer efficiency inside the composite and increases the overall mechanical properties. In particular, carbon fiber surfaces are inert, so the strength of the interface adhesion with resins is very weak. There are two main ways to strengthen the fiber-matrix adhesion of composite materials, and one is matrix modification. Yu *et al.*[17] improved the mechanical properties of CFRP by successfully distributing graphene nanoplatelets and multi-wiled carbon nanotube into epoxy resins. In particular, sample of two nanoparticles distributed on resin showed a 53.97% increased tensile strength over the base carbon fiber/epoxy composite. Lsitman *et al.*[19] added nanoclay to the PA6 resin, and produced a short glass fiber reinforced PA6 composite. According to the corresponding literature, the layers of the nanoclay acted as effective heterogenous nucleation sites, increasing crystallinity of PA6 and interfacial shear strength between fiber and matrix. Burn *et al.*[25, 42] conducted a study to improve the fiber-matrix adoption of composite materials using compatibilizer. he produced recycled short carbon fiber reinforced polypropylene composite, and improved 320% of interfacial shear strength by adding 2 wt.% of maleic anhydride-grafted polypropylene coupling agent into the resin.

Another method is surface treatment of the fiber. Fengie *et al.*[32, 43] introduced how to optimize the $H_3PO_4/H_2SO_4/HNO_3$ chemical oxidation method for surface treatment of carbon fiber. H_2SO_4 and HNO_3 increased oxidation on the surface of the fiber, while H_3PO_4 hindered the formation of defects on the turbostratic structure of carbon fibers via forming cycle structure with carbon-carbon bonds and prevented the carbon-carbon bonds from cleaving. In this way, the tensile strength was increased without damage to the carbon fiber. Veedu *et al.*[5] reinforced fiber-matrix adhesion by growing CNTs on the fiber surface. The chemical-vapor-deposition method was used to grow CNTs on the surface of the woven SiC fibers (**Fig. 2**a). Due to the CNTs forest grown through the thickness direction, the interlaminar fracture toughness, delamination resistance and in-plane mechanical properties were improved. In a similar study, BJ Kim[6] grew ZnO Nano-rods on a carbon fiber surface, then coated the fiber with CNT modified silane coupling agent (**Fig. 2**b). Through T-RTM process, we produced a multiscale hybrid composite. After the plasma treatment of the carbon fiber surface, the hydrothermal method was used to grow the ZnO Nano-rods without damage to the fiber surface,

ULSAN NATIONAL INSTITUTE OF SCIENCE AND TECHNOLOGY

and the CNT was coated on the surface by the silane coupling agent. The modified carbon fiber/A-PA6 composite showed a 159% improvement of in-plane shear strength.

In addition, Kim *et al.*[4, 6] used both methods to enhance the fiber-matrix adhesion. The T-RTM process was conducted with nanomaterial distributed resin and plasma-treated carbon fiber to make a nanomaterial-reinforced A-PA6/plasma-treated woven carbon fiber composite. As a result, mechanical tests showed improvement for all samples of nanomaterial added except for CNT, which was problem of CNT dispersion, and further increases by plasma treatment. In particular, exfoliated graphite nanoplatelet-reinforced A-PA6/plasma-treated carbon fiber composite had a highest improvement of in-plane shear strength.

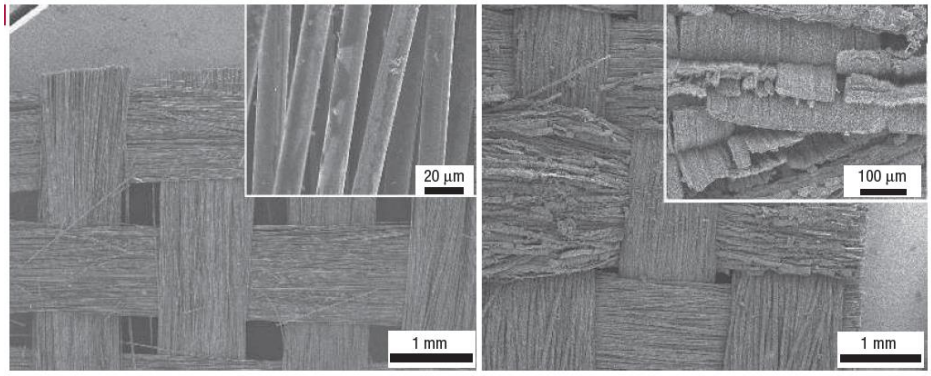

(a)

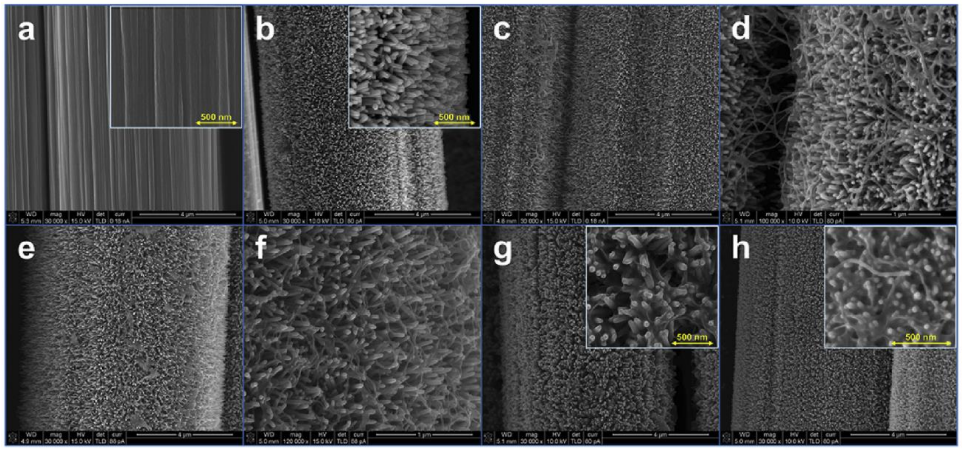

(b)

Figure 2. Various improvement methods for fiber-matrix adhesion: (a) the growth of CNTs on the SiC woven cloth[5], (b) ZnO nano-rods grown carbon fibers coated with CNT modified silane coupling agent[6].

ULSAN NATIONAL INSTITUTE OF SCIENCE AND TECHNOLOGY

2.3 Sizing Process

Coating of fiber surface using polymer is called sizing, and it will be covered separately in this part because they are closely related to the subject of the study. Sizing material coated on the fiber surface protects the brittle fiber from external damage, enhance the processability and fiber-matrix adhesion.

Usually, sizing materials coated on the surface of commercial carbon fiber are suitable for epoxy resin. Therefore, the compatibility of the carbon fiber is not sufficient with other types of resin. Gnadinger *et al.*[7] demonstrated the compatibility between resins and sizing materials (**Fig. 3**). When the commercial epoxy resin was used, composite samples made of carbon fiber coated with epoxy-based sizing material showed the highest interfacial shear strength (IFSS) increase. However, when thermoset polyurethane resin was used, the highest IFSS increase was shown in a composite sample made of carbon fiber coated with polyurethane based sizing material.

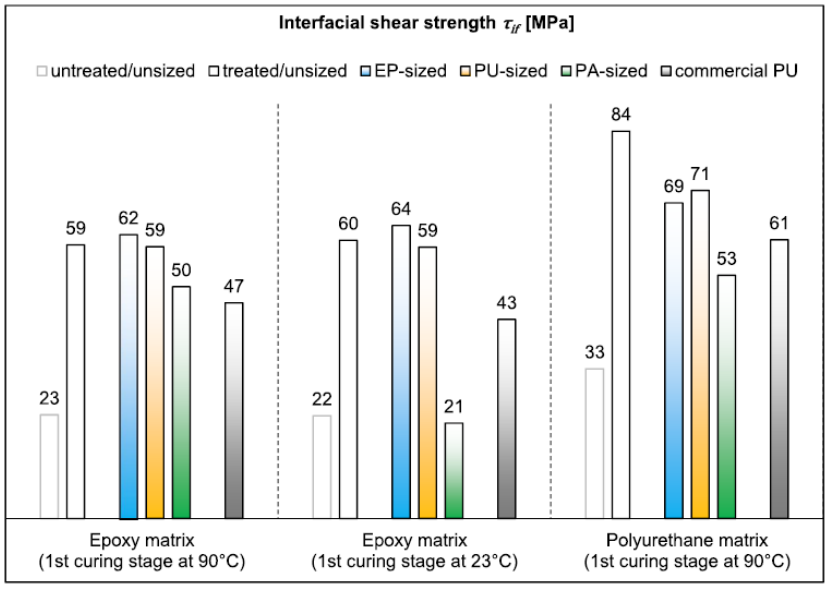

Figure 3. IFSS results of all investigated fiber-matrix combinations[7].

Sizing material acts as a coupling agent to increase the fiber-matrix adhesion. Liu *et al.*[29, 44, 45] produced sizing agent of emulsion type for carbon fiber, and demonstrated chemical reaction

ULSAN NATIONAL INSTITUTE OF SCIENCE AND TECHNOLOGY

of fiber/sizing/matrix with mechanical properties analysis of carbon fiber/vinyl ester composite. The HMSA-1 sizing agent, which was created, acted as a coupling agent by forming a covalent boning with the vinyl ester resin and functional groups on the carbon fiber surface, and interlaminar shear strength (ILSS) was improved by 20.7%.

Sizing process also allows the high performance and durability of composite materials to be used at high temperatures, such as parts of rocket engines. Allred *et al*.[8] improved fiber thermo-oxidative capability and mechanical performance through sizing on carbon fiber surface (**Fig. 4**). The sizing material coated on the commercial carbon fiber was removed and refinished it using the coupling agent and polyimide resin. After exposing it to a high temperature of 343°C, the results of mechanical tests showed that refinished sample had the least amount of microcracks, weight loss, and the strongest thermally stable interface.

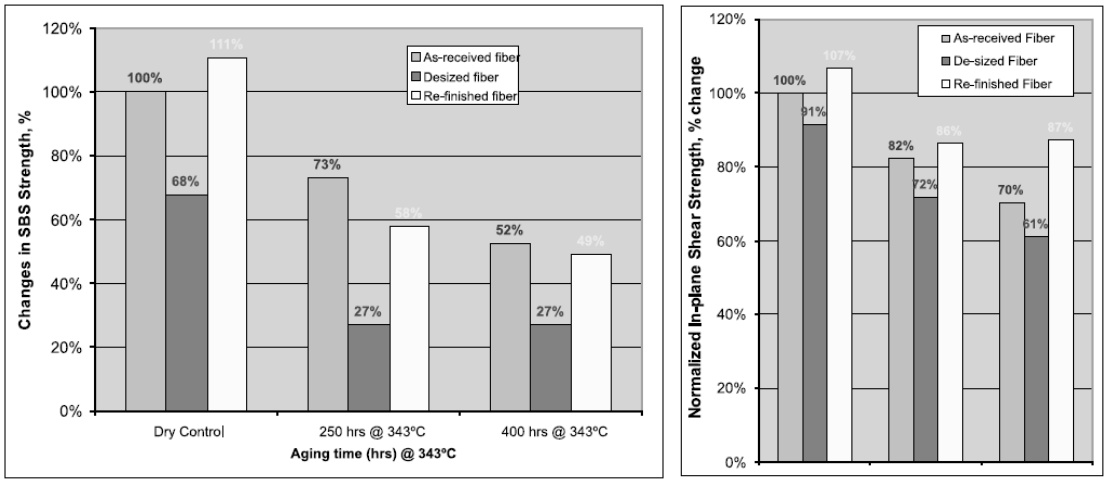

(a) (b)

Figure 4. Composite mechanical properties with different of fiber treatment and thermal aging condition: (a) short beam shear strength, and (b) in-plane shear strength[8].

In addition, surface energy changes due to sizing materials coated with carbon fiber affect fiber-matrix adhesion. Dai *et al*.[9, 46, 47] demonstrated the effect on surface energy changes and IFSS by desizing the commercial carbon fibers (**Fig. 5**). Using acetone extraction, the commercial carbon fiber coated with sizing material was desized, and following desizing

ULSAN NATIONAL INSTITUTE OF SCIENCE AND TECHNOLOGY

process, the dispersive component ratio of carbon fiber surface increased. A micro-droplet test using epoxy resin was conducted to measure IFSS. The result showed that desized-carbon fiber had a higher IFSS than the commercial carbon fibers, and it had a same tendency with the increase in dispersive component ratio of surface energy.

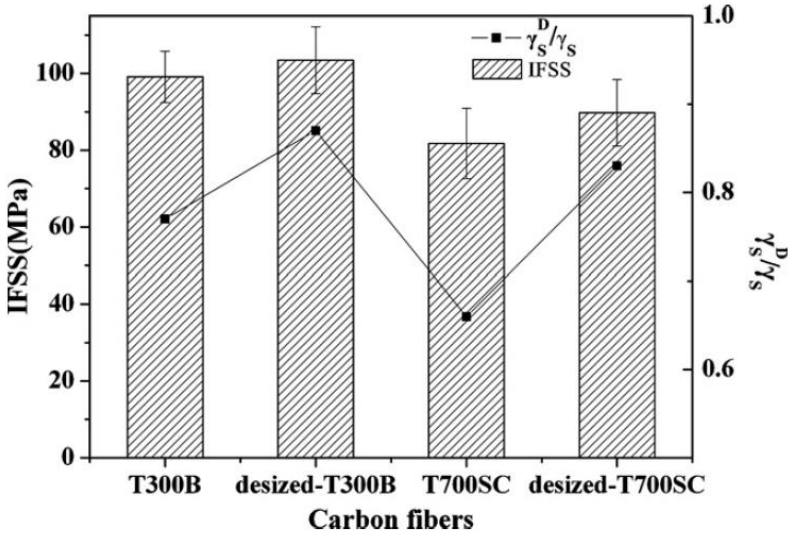

Figure 5. Interfacial shear strength of carbon fibers/epoxy and γ_S^D/γ_S [9].

ULSAN NATIONAL INSTITUTE OF SCIENCE AND TECHNOLOGY

3. Experimental

3.1. Materials

Commercial PAN-based 3k plain-woven carbon fibers (T-300, Toray, Japan) and uni-directional 24k non-woven carbon fibers (T-700, Toray, Japan) with epoxy sizing, and the ε-caprolactam (Caprolactam, Capro, Korea) were used as the primary materials. An activator (Addonyl® 8120, Rhein Chemie, Germany), a solid blocked diisocyanate, and a sodium-based catalyst (Addonyl® Kat NL, Rhein Chemie, Germany) were used for the anionic polymerization. For sizing materials, polyvinyl alcohol (PVA, 363138), polyethyele-graft-maleic anhydride (PE-g-MA, 456624), and (3-Aminopropyl)trimethoxysilane (AS, 281778) were supplied by Sigma-Aldrich. N-[5-(trimethoxysilyl)-2-aza-1-oxopentyl]caprolactam coupling agent (CPLS, SIT8394.0) was purchased from Gelest, Inc. Anionic polyamide dispersion (PA, Hydrosize® PA874), epoxy dispersion (EP, Hydrosize® EP876), polyurethane dispersion (PU, Hydrosize® U501) were purchased from Michelman (Cincinnati, United States)

ULSAN NATIONAL INSTITUTE OF SCIENCE AND TECHNOLOGY

3.2. Sample Preparation

3.2.1. Desizing Process

Commercial carbon fibers have already coated surfaces with sizing materials, mainly epoxy type. The existing coated sizing material was desized to evaluate the effects of the sizing materials. Lee *et al*.[48] removed sizing material of commercial carbon fiber by acetone washing at room temperature. This is a safe and simple method because it does not use any strong solvents or heating process. In a same way, we put the commercial woven carbon fiber in the acetone. The following TGA result (**Fig. 6**) confirmed that sizing material on the commercial carbon fiber was degraded at 200℃. 24 hours after dipping acetone, almost degradation was not found, and 72 hours later, the coating was completely eliminated.

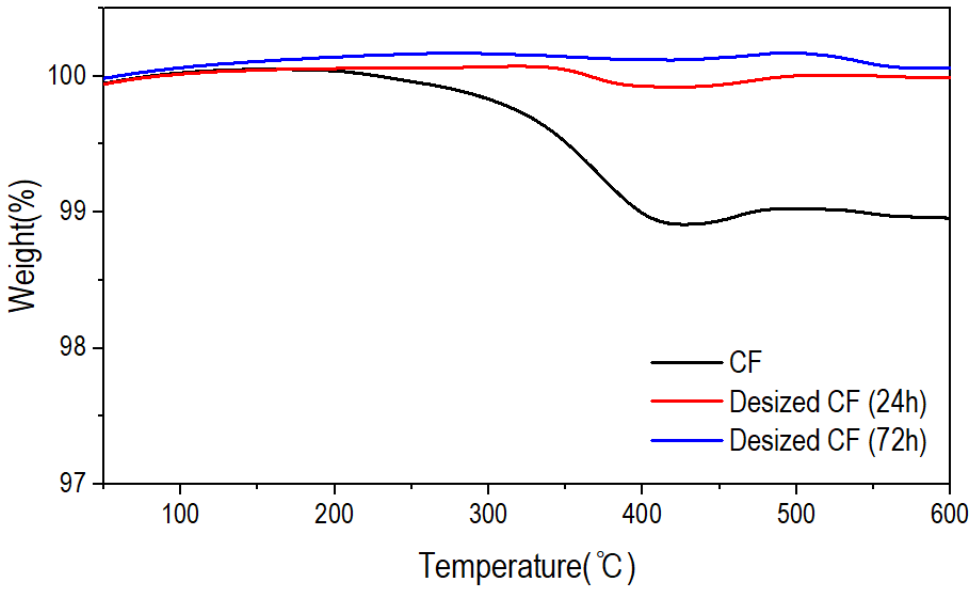

Figure 6. TGA curves of desized carbon fibers with different dipping time in acetone.

ULSAN NATIONAL INSTITUTE OF SCIENCE AND TECHNOLOGY

3.2.2. Sizing Process

Next, desized carbon fiber was coated with sizing materials. First, we wetted the woven carbon fiber in a sizing solution designed for each sizing material for one minute, then removed and heat it in an oven. Weight of carbon fiber before and after the sizing process was measured at least five times to calculate the sizing content. The concentration of sizing materials, heat treatment temperature and time were optimized for each sizing material to achieve a suitable sizing content of 1 to 1.5 wt.%, and the result is shown in the **Table 1**.

Table 1. Optimization results of sizing process for each sizing materials.

Sizing material		PVA[49, 50]	AS[51, 52]	CPLS[53]	PE-g-MA[54]	PU[55]	PA[55]	EP[55]
Sizing solution	*Solvent	DI	M+DI	M+DI	Toluene	DI	DI	DI
	Concentration (wt.%)	0.75	1	2	1	1.5	3	1.5
Heat treatment	Temperature (℃)	90	80	100	110	160	180	160
	Time (min)	120	120	240	60	5	5	5
Sizing content (wt.%)	Average	1.22	1.34	1.49	0.91	1.14	1.15	1.43
	Standard deviation	0.02	0.12	0.06	0.08	0.02	0.13	0.10

* DI – DI-water, M+DI – 95% of methanol and 5% of DI-water

ULSAN NATIONAL INSTITUTE OF SCIENCE AND TECHNOLOGY

3.2.3. T-RTM Process

Finally, a coated carbon fiber reinforced A-PA6 composite was manufactured using a T-RTM process. Coated carbon fiber fabrics were placed inside the mold, then catalyst (3.7 wt.%) and activator (2.9 wt.%) with ε-caprolactam were melted in the individual tanks A and B that maintain nitrogen environment. After the temperature of the mold reached a suitable processing temperature of 145℃, the matrix solutions in individual tanks A and B were immediately mixed and transferred into the mold using vacuum (75 kPa). The polymerization was completed within 25 seconds. **Figure 7** Shows the schematics of sizing process and T-RTM.

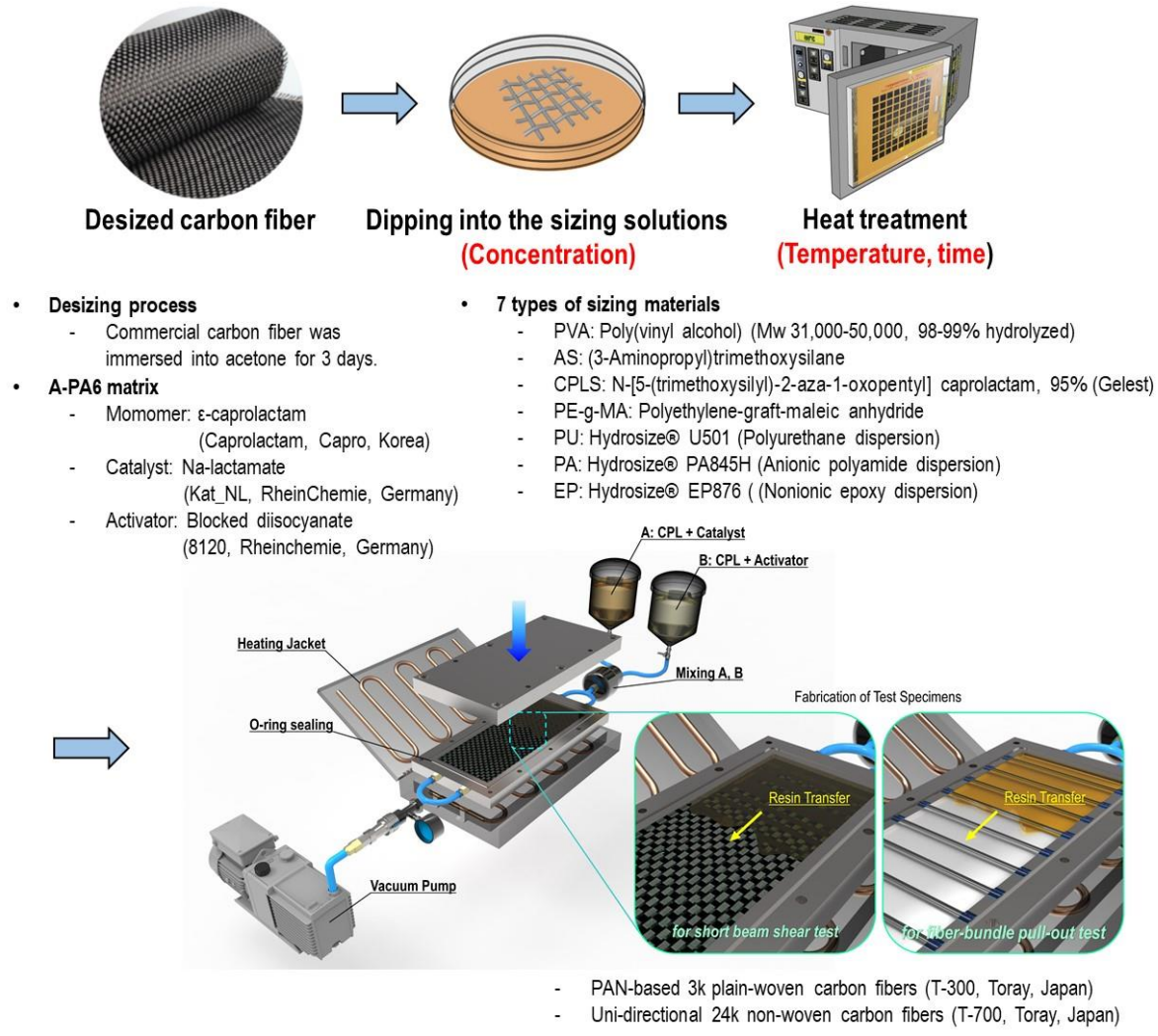

Figure 7. Processing schematics of sizing and T-RTM processes.

ULSAN NATIONAL INSTITUTE OF SCIENCE AND TECHNOLOGY

3.3. Characterization and Mechanical Testing

The thermal degradation of sizing materials on the carbon fiber was investigated using a thermogravimetric analysis (TGA, Q500, TA instruments). The measurement was performed from 50℃ to 600℃ with heating rate of 10℃/min under nitrogen atmosphere. The morphology of coated carbon fiber surface and fracture surface was investigated using a high-resolution scanning electron microscopy (HR-SEM, Nano-nova 230, FEI). The surface composition of sizing materials-coated carbon fiber was characterized using a X-ray photoelectron spectroscopy (XPS, K-Alpha, Thermo Fisher Scientific). The XPS spectra were obtained using an Al Kα monochromatic X-ray source (1486.6 eV).

For the contact angle measurement, a capillary rise method[56-58] was used with KRÜSS k100 tensiometer equipment. The coated woven carbon fibers were measured by grinding finely into a fiber chamber. Contact angles θ were calculated using Eq. 1:

$$\frac{m^2}{t} = \frac{c \cdot \rho_L^2 \cdot \sigma_L \cdot cos\theta}{\eta_L} \quad (1)$$

where m is the mass of the absorbed solvent, t is absorption time, c is the capillary constant of each fiber, ρ_L is the density of the measuring solvent, σ_L is the surface energy of the measuring solvent and η_L is a dynamic viscosity of measuring solvent.

A total of four solvents, distilled water, diiodomethane, toluene and n-hexane, were used to measure contact angles of each samples and each surface energy was calculated using the Owens, Wendt, Rabel and Kaelble method[59, 60] in the following Eq. 2:

$$\frac{\sigma_L \cdot (\cos\theta + 1)}{2 \cdot \sqrt{\sigma_L^D}} = \sqrt{\sigma_S^P} \cdot \frac{\sqrt{\sigma_L^P}}{\sqrt{\sigma_L^D}} + \sqrt{\sigma_S^D} \quad (2)$$

The superscripts P and D refer to the polar and the dispersive component, and subscripts S and L refer to the solid samples and the measuring solvent.

To evaluate mechanical properties of the composite materials, fiber-bundle pull-out test[61]

ULSAN NATIONAL INSTITUTE OF SCIENCE AND TECHNOLOGY

and the short beam shear test were performed. IFSS and short beam strength of composites were measured by a universal testing machine (UTM, 5982, Instron). In the fiber-bundle pull-out test, one end of the 24k carbon fiber bundle (T-700) was embedded inside the A-PA6 matrix and embedded length is 3~5 mm. An experiment was performed with 0.5 mm/min crosshead speed, and the specimen was measured at least 10 times per sample. IFSS [MPa] was calculated using Eq. 3:

$$\mathrm{IFSS} = \frac{F_P}{2 \cdot (W_b + H_b) \cdot L_e} \tag{3}$$

where F_P is maximum load [N], W_b, H_b and L_e are width [mm], height [mm] and length [mm] of the embedded bundle fiber.

In the short beam test, specimen information and test method were obtained from ASTM D2344 standard. The test specimen has 24 mm length, 8 mm width and 4 mm height and 20 plies of woven carbon fiber fabrics (T-300) were used. The measured fiber volume fraction is approximately 50%. The test was performed at least 10 times for each sizing materials with a crosshead speed of 1 mm/min. Short beam stress when displacement of crosshead was 4 mm was defined as “short beam strength” in this paper. Short beam strength [MPa] was calculated using Eq. 4:

$$\text{Short beam strength} = 0.75 \cdot \frac{F_P}{b \cdot h} \tag{4}$$

where F_P is the load at 4 mm of crosshead displacement [N], b and h are specimen width [mm] and specimen thickness [mm] of the composite samples.

The chemical reactions between sizing materials and A-PA6 matrix were investigated by analyzing the specific peaks using FT-IR spectroscopy (Nicolet™ iS50, Thermo Fisher Scientific Inc., USA). For ATR-FTIR measurements, Nicolet™ iS50 was equipped with a Smart MIRacle™ (PIKE Technologies, Inc., USA) ATR module. A Germanium crystal (18 mm diameter) was used, and sizing materials/A-PA6 polymer composites were analyzed in transmittance mode over the scanning range 650 - 4000 cm^{-1} at room temperature.

X-ray micro CT measurements were performed to measure internal void content of

ULSAN NATIONAL INSTITUTE OF
SCIENCE AND TECHNOLOGY

composites using a SkyScan 1176 desk-top X-ray microscanner (Bruker, Belgium). Microfocus sealed X-ray tube was operated at 40 kV/400 μA, and resolution of the scanning was 9 μm. To calculate the void content of the composite, CTAn and CTVol, 2D/ 3D processing and analysis programs of Bruker, were used with the constant threshold value determined by optical comparison[62]. A volume for void analysis of the composites is $8 \times 8 \times 1.5$ mm.

ULSAN NATIONAL INSTITUTE OF SCIENCE AND TECHNOLOGY

4. Results and Discussion

4.1. TGA of Coated Carbon Fiber

TGA was performed to analyze the thermal stability of sizing materials coated on the carbon fiber. If the sizing material is degraded during the composite manufacturing process, not only does it lose its effect of the sizing process, but also the gas generated from the degradation can form a void inside the composite.[63] The TGA results are shown in **Fig. 8**. In the case of CPLS- and EP-CF, weight loss occurred at 190 ℃ which was lower than others. However, since the process temperature of T-RTM is relatively low (~170 ℃) by using catalyst and activator, all seven sizing materials can be used in the T-RTM process without degradation.

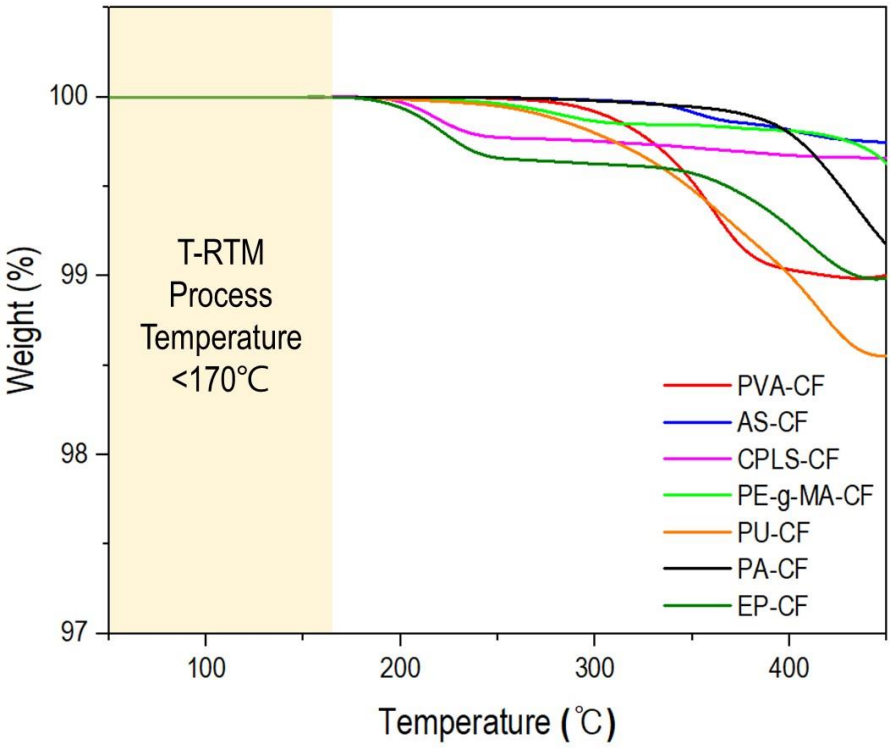

Figure 8. TGA curves of carbon fibers coated with different sizing materials.

ULSAN NATIONAL INSTITUTE OF SCIENCE AND TECHNOLOGY

4.2. SEM Morphological Analysis of Coated Carbon Fiber

Next, the surface morphology of the coated fiber was analyzed using SEM, and **Fig. 9** shows SEM micrographs of desized-CF and coated CFs. The surface curvature of desized-fiber was softened by sizing materials evenly coated on the fiber surface. In particular, the sizing process was carried out by putting woven carbon fiber sheets rather than filaments commonly used, but trapped area of sizing materials between the filament was not found. There were no noticeable roughness differences of carbon fiber surface depending on the sizing materials, and it referred no mechanical interlocking effect by sizing.

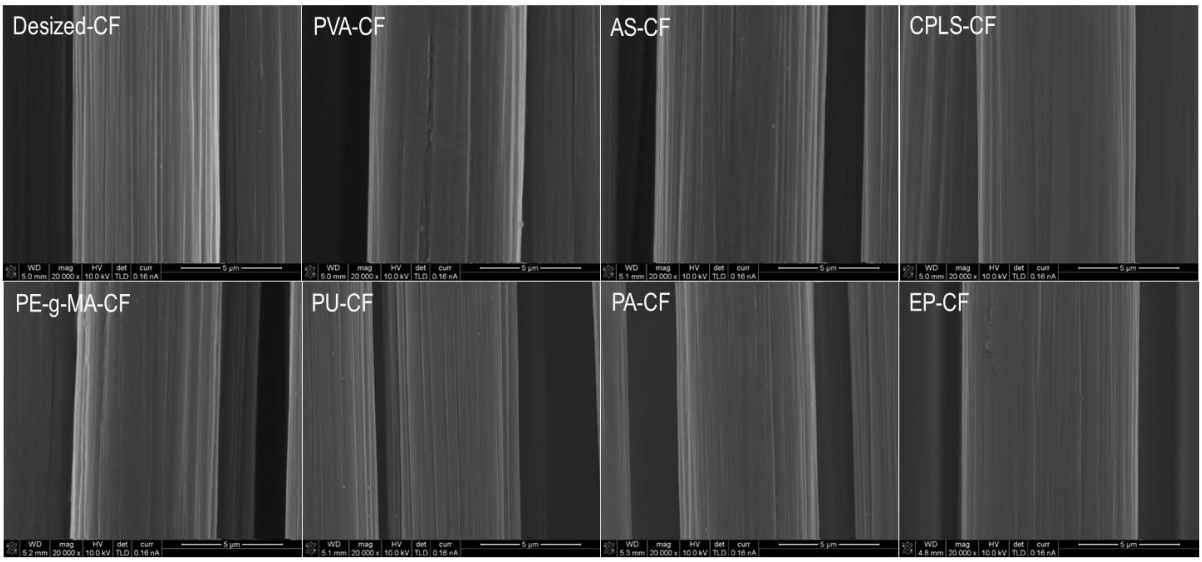

Figure 9. SEM micrographs of carbon fibers with different sizing materials.

ULSAN NATIONAL INSTITUTE OF SCIENCE AND TECHNOLOGY

4.3. XPS Analysis of Coated Carbon Fiber

The XPS analysis was performed to investigate the chemical composition and functional groups of the coated carbon fiber surface. First, the chemical composition of the carbon fiber surface changed with the sizing materials, and it is shown in **Table 2**. For AS-CF, CPLS-CF, and PA-CF, the nitrogen ratio increased compared to the desized-CF and the Si was detected for samples coated with silane coupling agent. Since PE-g-MA-CF was coated with PE based copolymer, a non-polar polymer, the oxygen ratio was greatly reduced.

Table 2. Elemental compositions of carbon fiber coated with different sizing materials.

Samples	C (%)	N (%)	O (%)	Si (%)
Desized-CF	78.86	0.79	18.13	-
PVA-CF	80.12	0.16	19.43	-
AS-CF	72.96	2.49	17.46	4.69
CPLS-CF	68.79	7.20	19.05	4.96
PE-g-MA-CF	89.03	0.95	7.68	-
PU-CF	79.3	1.31	18.49	-
PA-CF	80.35	1.48	17.19	-
EP-CF	77.38	-	20.80	-

The C 1s peak spectrum of the coated carbon fiber surface was deconvolved into several Gaussian-Lorentzian (8:2) peaks[6, 64-67] by CasaXPS program, and the results were shown in the **Table 3** and **Fig. 10**. Small amounts of functional groups were shown even in the desizied-CF sample, it means desizing process in acetone did not completely remove the sizing of commercial carbon fiber. Then, depending on the sizing materials, the functional groups related to the sizing material were found in the samples. In the case of PVA-CF, the amount of hydroxyl group (-OH) compared to desized-CF increased significantly, as PVA has numerous hydroxyl groups in the structure. For CPLS-CF, a significant increase in peak value of 289.4 eV was related to the carboxylic acid (COOH) groups. This shows that the ring structure of CPLS was

ULSAN NATIONAL INSTITUTE OF SCIENCE AND TECHNOLOGY

opened during sizing process and the ε-aminocaproic acids were formed[68]. PE-g-MA-CF had very small amounts of functional groups because PE is non-polar. Although it was grafted by maleic anhydride, the ratio was also very low (~0.5 wt.%). In the case of EP-CF, the peak 3 corresponding to the epoxide group was found to have increased compared to desized-CF.

The sum of area percent from peak 2 to peak 6 refers carbon atoms conjunct with the oxygen or nitrogen that can be react with the matrix, and is called activated carbon percent[64, 65], excluding peak 1 indicating C-C bonding. PVA-CF, EP-CF and PA-CF showed high increases compared to desized-CF, and PE-g-MA-CF significantly decreased. Based on the XPS analysis results, it was expected that PVA-CF, EP-CF, and PA-CF would undergo active chemical interactions with the A-PA6 resin.

Table 3. C(ls) Peaks of coated carbon fibers and relative peak areas.

Samples	C(1s) peaks in different states B.E., Ev (area, %)						
	Peak 1 285.0eV	Peak 2 286.5eV	Peak 3 287.1eV	Peak 4 287.7eV	Peak 5 289.4eV	Peak 6 290.6eV	Activated carbon(%)
Desized-CF	69.54	17.51	8.60	2.81	0.76	0.77	30.45
PVA-CF	60.42	34.01	4.18	0.45	0.04	0.90	39.58
AS-CF	74.51	15.81	6.28	2.71	0.70	-	25.50
CPLS-CF	74.73	16.70	-	0.44	8.12	-	25.26
PE-g-MA-CF	94.36	2.83	2.82	-	-	-	5.65
PU-CF	64.84	28.93	3.17	1.55	1.46	0.05	35.16
PA-CF	60.44	29.04	5.53	3.47	0.12	1.40	39.56
EP-CF	54.64	34.14	10.56	0.65	-	-	45.35
Peak assignment	-C-C -C-H	-C-OH -C-O-C -C-N	*C-O-C=O Epoxide group	-C=O -C=N -N-C=O	-COOH -COOR	$-COO^-$ π–π*	

ULSAN NATIONAL INSTITUTE OF
SCIENCE AND TECHNOLOGY

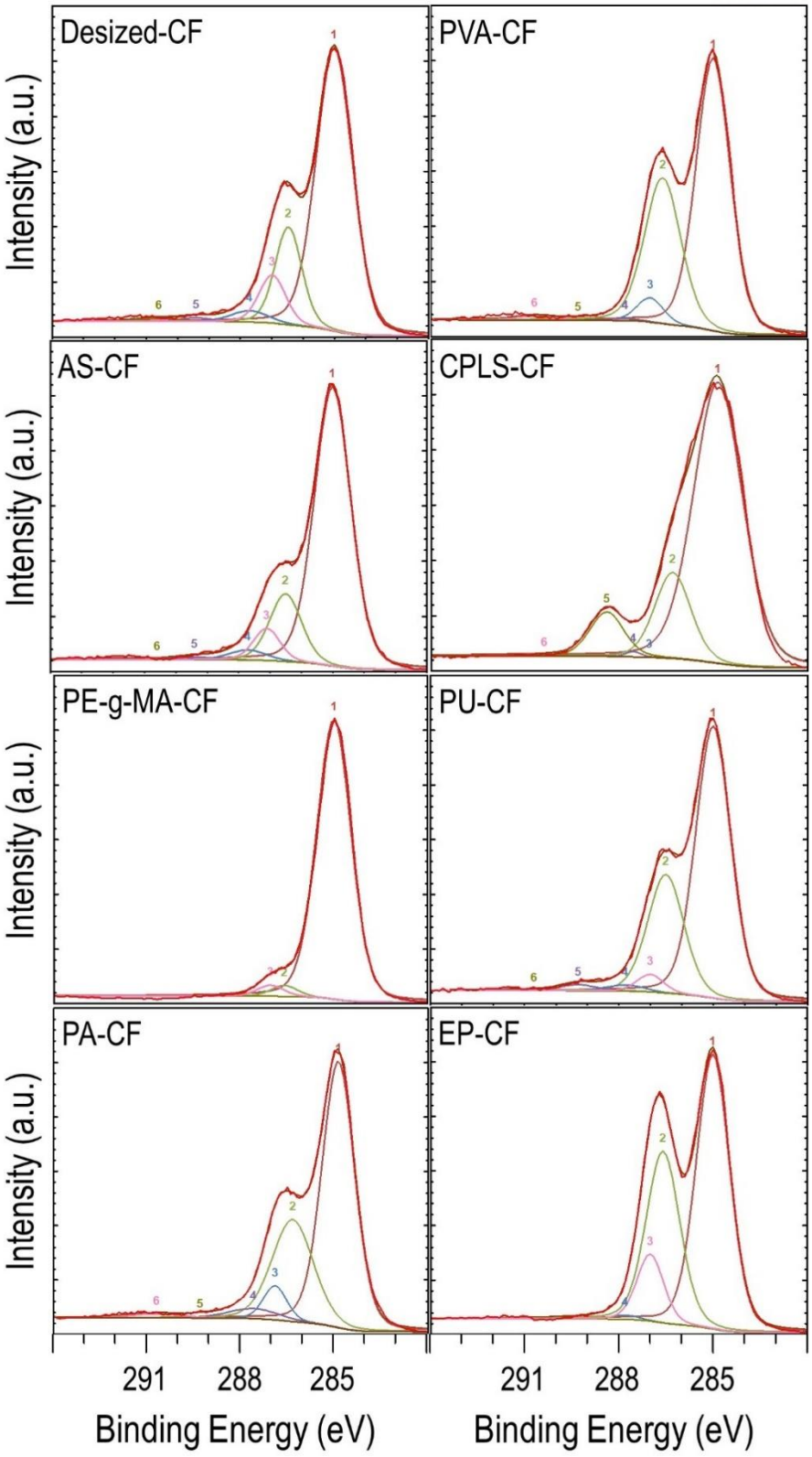

Figure 10. Deconvoluted C1s spectra of coated carbon fiber surfaces with different sizing materials.

ULSAN NATIONAL INSTITUTE OF SCIENCE AND TECHNOLOGY

4.4. Surface Energy Analysis

Surface energy is an important factor in studying the fiber/matrix adhesion of composite materials. Total surface energy and polar/dispersive component ratio of fiber are related to the matrix impregnability inside the fabrics, and consequently affect the properties of the composite[69-73]. In particular, for high-speed manufacturing processes such as T-RTM, the overall processing time is very short. Thus, the wettability of the fibers affects the process parameters. The result of surface energy was shown in the **Table 4**. EP-CF and PA-CF showed an increase in total surface energy γ_s compared to desized-CF, and a significant decrease in PE-g-MA-CF and CPLS-CF. Based on the polar component ratio γ_s^p/γ_s, PA-CF, EP-CF, and PVA-CF increased compared to desized-CF, and PE-G-MA-CF and PU-CF showed decreases. This is consistent with the previous analysis of XPS results, except for PU-CF. It means that the increase of activated carbon percent indicates an increase of polar component on carbon fiber surfaces[58]. In addition, A-PA6 matrix has high polar component ratio due to hydrogen bonding of the amide group. When compared with the results of coated carbon fiber and matrix, EP-CF and PA-CF are suitable for T-RTM process due to high surface energy and the polar component ratio.

Table 4. Surface energies of desized, coated carbon fibers, and A-PA6 matrix.

Surface energy (mJ/m²)	Desized-CF	PVA-CF	AS-CF	CPLS-CF	PE-g-MA-CF	PU-CF	PA-CF	EP-CF	A-PA6
Polar component (γ_S^P)	24.7	28.6	17.6	13.4	9.3	12.6	35.9	41.4	19.5
Dispersive component (γ_S^D)	42.4	36.8	33.3	27.6	27.8	37.5	38.0	28.9	37.3
Total surface enenrgy (γ_S)	67.1	65.4	50.9	41.0	37.1	50.1	73.9	70.3	56.8
γ_S^P/γ_S	0.37	0.44	0.35	0.33	0.25	0.25	0.49	0.59	0.34

ULSAN NATIONAL INSTITUTE OF SCIENCE AND TECHNOLOGY

4.5. Fiber-Bundle Pull-out Test

To measure the interfacial shear strength, the fiber-bundle full-out test was conducted. In the case of A-PA6 where polymerization process is sensitive to moisture, there are a lot of difficulties in existing tests such as micro-droplet test, single fiber full-out test and fragmentation test. Thus, the research has been conducted to measure IFSS by replacing a filament with a bundle[74, 75]. In particular, since this study conducted sizing process with form of woven carbon fiber fabric, the fiber-bundle full-out test was more effective to evaluate the sizing effects. Zhou *et al.* introduced a fiber-bundle pull-out test, and reliability of the test was investigated according to different filament test conditions[61]. In addition to its high reliability, it was closely related to the ILSS results. Thus, in this study, IFSS was measured by referring to the fiber-bundled pull-out test method in the corresponding literature.

The results are then shown in **Fig. 11**. It was confirmed that most of the coated CF/A-PA6 composites had higher IFSS than the desized-CF/A-PA6 composite. PVA-CF/A-PA6, AS-CF/A-PA6 and PE-g-MA-CF/A-PA6 showed slight improvement over desized-CF/A-PA6. In the case of PVA-CF/A-PA6, XPS and surface energy results showed a high percent of activated carbon, total surface energy and polar component ratio, but there was not much improvement than desized-CF/A-PA6. PE-g-MA-CF/A-PA6 showed a slight increase in IFSS despite having very lower activated carbon percent, total surface energy and polar component ratio. For AS-CF/A-PA6, IFSS increased about 17.2%, although there was no noticeable difference with the desized-CF in the previous analysis. The highest improvement was approximately 30% increases in PA-CF/A-PA6 and EP-CF/A-PA6. On the contrary, IFSS of CPLS-CF/A-PA6 and PU-CF/A-PA6 decreased about 20%.

ULSAN NATIONAL INSTITUTE OF
SCIENCE AND TECHNOLOGY

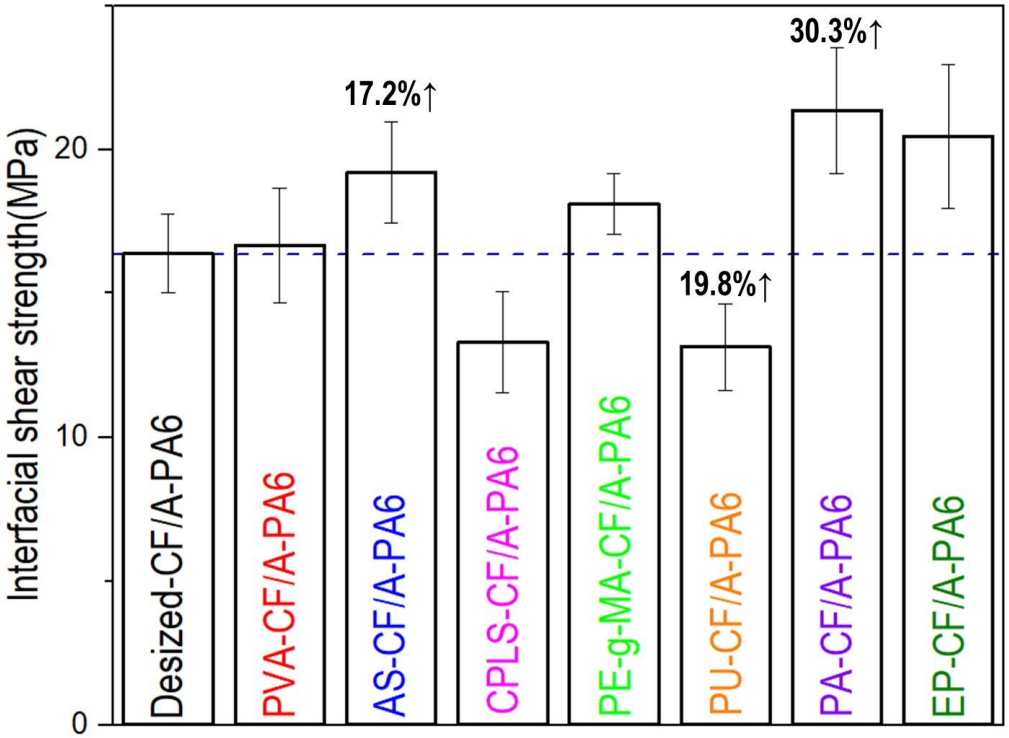

Figure 11. Interfacial shear strength of coated carbon fiber/A-PA6 composites.

ULSAN NATIONAL INSTITUTE OF SCIENCE AND TECHNOLOGY

4.6. Short Beam Shear Test

To measure short beam strength of the composite, short beam shear test was conducted according to ASTM 2344 standard. The span-to-thickness ratio of the specimen is intentionally relatively small. For such short beam shear test, the bending stresses produced in the specimen are reduced, and thus the shear stresses in the specimen are significance. Under three-point loading, these shear stresses do not vary across the span length but do vary parabolically through the thickness. As a result, these shear stresses in the central region of the specimen thickness will produce an interlaminar shear failure. However, because thermoplastic composites are ductile, a combination of flexure and inelastic deformation failure occurs with delamination failure. In load-displacement curves below (**Fig. 12**), load continues to increase with increasing of crosshead displacement, which is why it is impossible to define the interlaminar shear strength of the CFRP produced in this experiment. Therefore, "short beam strength" was defined as short beam stress when the crosshead displacement is 4mm which is thickness of the specimen. The results are then shown in **Fig. 12**. Short beam strength results were very similar to IFSS results. For PVA-CF/A-PA6, AS-CF/A-PA6 and PE-g-MA-CF/A-PA6, it slightly increased and the short beam strength of PU-CF/A-PA6 slightly decreased. EP-CF/A-PA6 and PA-CF/A-PA6 showed the highest increase of short beam strength about 60%, and the value of CPLS-CF/A-PA6 decreased 25%.

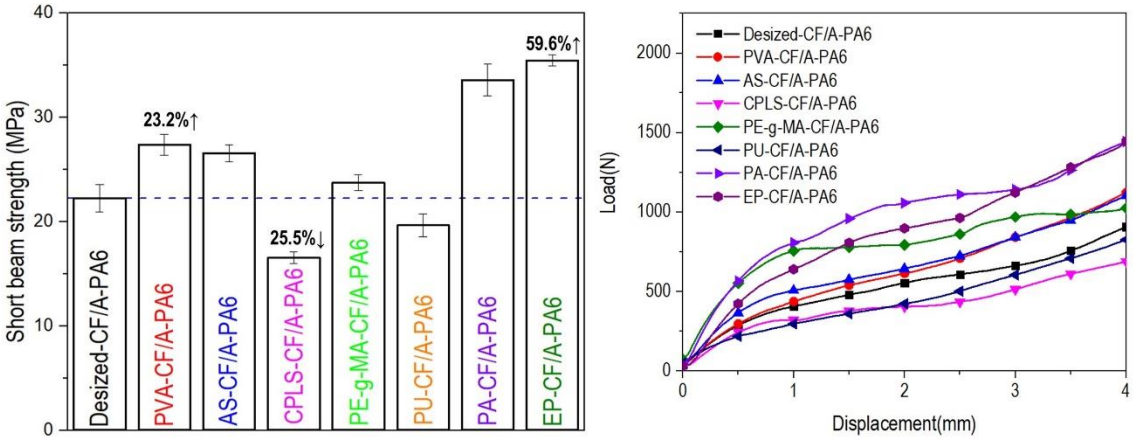

Figure 12. Short beam strength and load-displacement curves of coated carbon fiber/A-PA6 composites.

ULSAN NATIONAL INSTITUTE OF SCIENCE AND TECHNOLOGY

Figure 13 shows the results of IFSS and short beam strength in one graph. First, there was a very close trend in IFSS and short beam strength, which showed that short beam strength is closely related with IFSS. In addition, the difference in the results of short beam strength was more pronounced than in IFSS, indicating that interlaminar interface strengthening was more prominent as the scale increases from a bundle to woven fibers. PA-CF/A-PA6 and EP-CF/A-PA6 showed the highest improvement in two mechanical tests. This has same tendency with the results of XPS and surface energy, indicating that activated carbon percent and surface energy of fiber have a significant effect on fiber-matrix adhesion of the composite materials. For CPLS-CF/A-PA6, although the caprolactam ring structure of CPLS was expected to have chemical interactions actively with the A-PA6 resin, both mechanical tests had the lowest results, even decreased than desized-CF/A-PA6. The results of the previous analysis, XPS and surface energy, could not fully explain the results of mechanical tests because not only physical wetting but also chemical reactions of sizing/A-PA6 is important to analyze improvement mechanism of fiber-matrix adhesion. The possible chemical reactions between sizing materials and A-PA6 resin were analyzed and the FT-IR analysis was performed to confirm that.

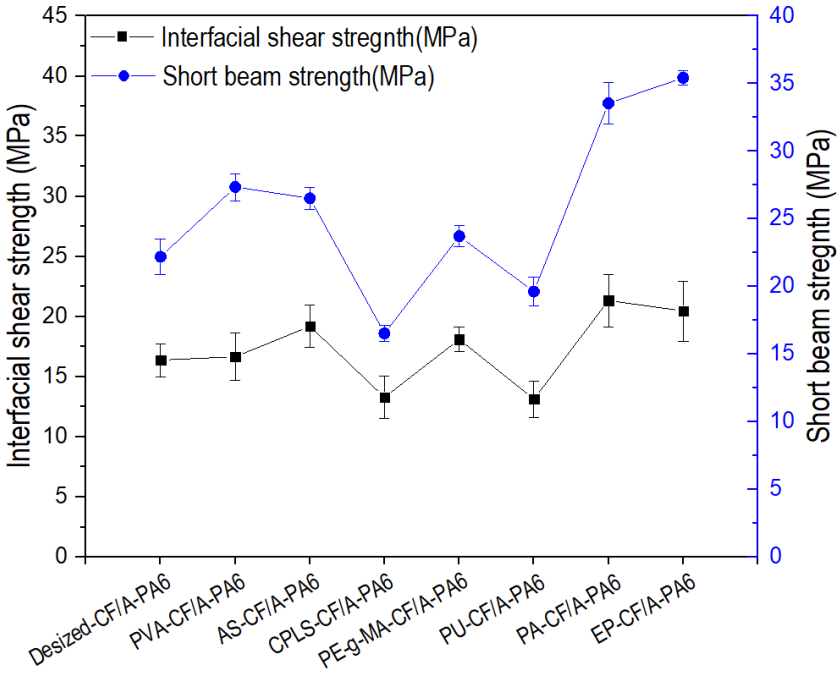

Figure 13. Interfacial shear strength and short beam strength of coated carbon fiber/A-PA6 composites.

ULSAN NATIONAL INSTITUTE OF SCIENCE AND TECHNOLOGY

4.7. Reinforcement Mechanism

4.7.1. Anionic Ring Opening Polymerization of ε-caprolactam

The mechanism of anionic ring opening polymerization[76] of ε-caprolactam is shown in **Fig. 14**. The initiator is anions of the ε-caprolactam itself and is formed by a small amount of sodium hydride. The anion of the caprolactam attacks ε-caprolactam molecule of blocked diisocyanate and extracts a proton, opening the ring and generating a new amide anion. The anion then extracts a proton from a fresh ε-caprolactam, generating a new ε-caprolactam anion. The ring-carbonyl carbon is now strongly activated towards nucleophilic attack, and so is rapidly attacked by the newly formed ε-caprolactam anion. The resulting amide anion deprotonates a further molecule of ε-caprolactam, which can then attack the ring-carbonyl, thus leading to continued ring-opening polymerization.

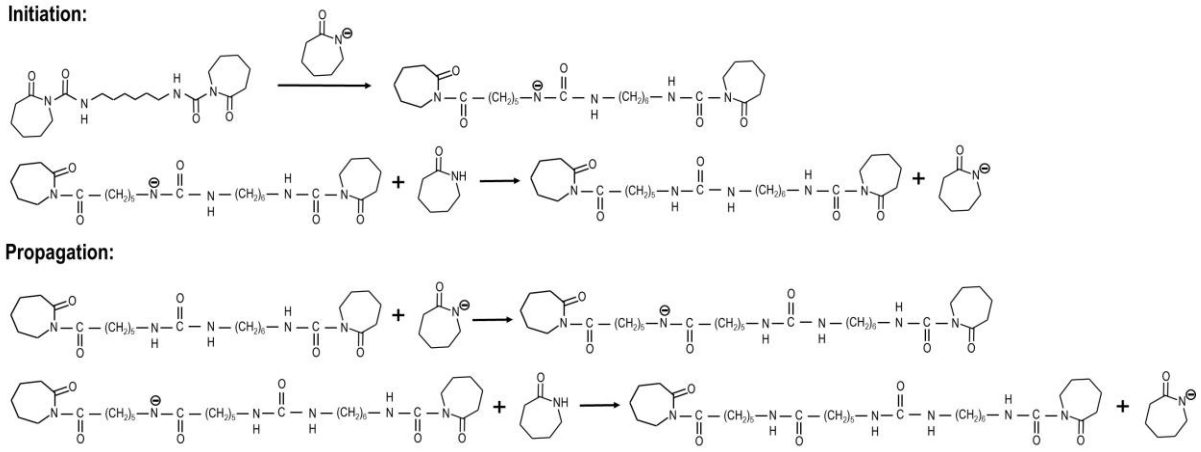

Figure 14. The anionic ring opening polymerization of ε-caprolactam

ULSAN NATIONAL INSTITUTE OF SCIENCE AND TECHNOLOGY

4.7.2. Chemical Reactions of Sizing Materials/A-PA6

The possible chemical reactions between sizing materials and A-PA6 matrix during T-RTM process are shown in the **Fig. 15**. In the case of PVA[77, 78] (**Fig. 15**a), it does not form a covalent bonding with A-PA6 through chemical reactions without catalyst or high temperature process. Hydroxyl groups of PVA form a strong hydrogen bonding with amide/carbonyl groups of A-PA6. The isocyanate group, for AS[79] (**Fig. 15**b), is created during the A-PA6 polymerization because the process temperature is higher than the de-block temperature of the activator. The amine group of AS and isocyanate group from the activator form the urea linkage. For CPLS[53] (**Fig. 15**c), it has a ε-caprolactam ring which is a monomer of A-PA6 matrix. Thus, it reacts with ion form of catalyst and participates in the polymerization, forming A-PA6 chain. Maleic anhydride group of PE-g-MA (**Fig. 15**d) and catalyst Na-lactamate react to create covalent bonding, and participate in the polymerization, forming an A-PA6 chain[80].

In case of PU[81] (**Fig. 15**e), the urethane group is dissociated by reaction with the melt caprolactam solution, which is weak alkaline condition at high temperature, and consequently the isocyanate group and hydroxyl group are produced. With anion of ε-caprolactam, the isocyanate group reacts rapidly with ε-caprolactam, and forming the PA6 chain in the A-PA6 polymerization. PA sizing material is polymer composed of the repeated amide groups like A-PA6 matrix, which forms a strong hydrogen bonding between them (**Fig. 15**f). Lastly, EP[82] (**Fig. 15**g) reacts with the amide group of A-PA6, and forming a covalent bonding. The reaction is a nucleophilic attack on the oxirane ring by the amide nitrogen of polycaprolactam.

ULSAN NATIONAL INSTITUTE OF SCIENCE AND TECHNOLOGY

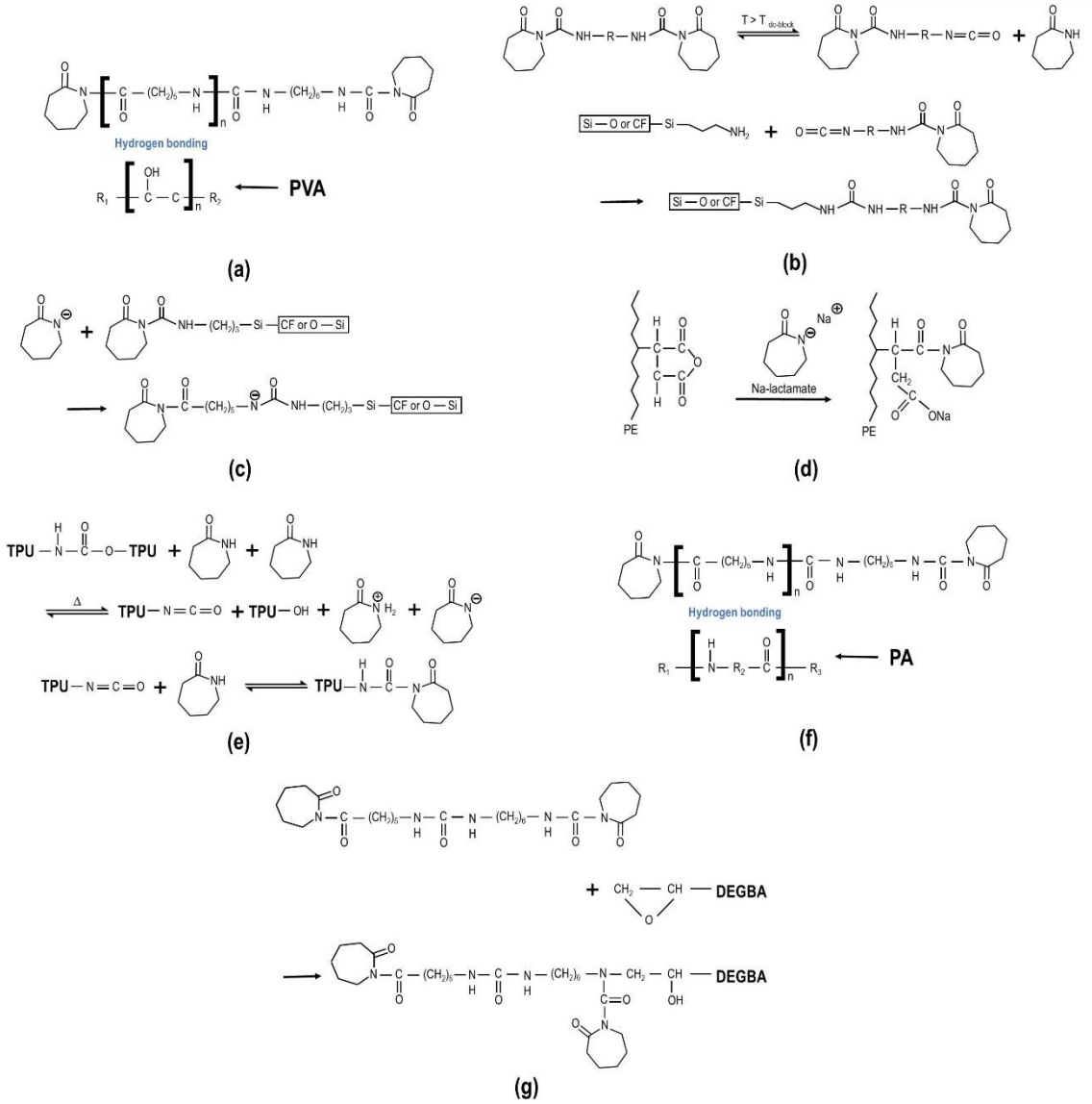

Figure 15. Reactions of sizing materials and ε-caprolactam during polymerization.

ULSAN NATIONAL INSTITUTE OF SCIENCE AND TECHNOLOGY

4.8. FTIR Spectroscopy of Sizing Materials/A-PA6

The FT-IR analysis was performed with sizing materials/A-PA6 polymer composites, and the sizing materials were used in the same conditions as the sizing process before analysis. All results are shown in **Fig. 16**. First, in the case of PVA, a broad O-H peak was identified at 3333 cm^{-1}. Similarly, the O-H, amide I and II peaks were confirmed in PVA/A-PA6, which showed the potential in which the amide group of A-PA6 and the hydroxyl group of PVA form a hydrogen bonding at the fiber interface. In the results of AS, the peaks related to Si bonding were observed to be large, 1099 cm^{-1} (Si-O-C stretching), 1018 cm^{-1} (Si-O-Si, asymmetric stretching), 926 cm^{-1} (Si-OH, stretching), 863 cm^{-1} (Si-O-Si, symmetric stretching). Weak amine group was identified. 3357 cm^{-1} (N-H, stretching), 1594 cm^{-1} (N-H, bending), 690 cm^{-1} (N-H, out of plane bending). As a result, it is confirmed that condensation reaction occurred during the sizing process and Si-O-Si bonding was actively observed on the surface. It can be expected that the chemical reaction of A-PA6 resin and AS during the polymerization process as mentioned above.

The result of CPLS showed prominent peaks at 1701 cm^{-1}, 1084 cm^{-1} and 805 cm^{-1}, respectively representing stretching vibrations of the C = O, Si-O-Si asymmetric stretching and Si-O-Si symmetric stretching. Through this, ε-caprolactam ring structure, silane hydrolysis, condensation reaction was confirmed. In addition, it is confirmed that the ring structure of ε-caprolactam was opened and the ε-aminocaproic acid was formed during the sizing process by 3282 cm^{-1} O-H stretching, 3275 cm^{-1} N-H stretching and 1175 cm^{-1} stretching of C-O peaks. In CPLS/A-PA6, the peaks of Amide I and II were observed as in A-PA6, and the carbonyl peak was shifted to a lower wavenumber, indicating the participation of ε-caprolactam structure of CPLS in the polymerization reaction. PE-g-MA was found to have peaks related to polyethylene, 2919 cm^{-1} (sp^3 C-H stretching), 1462 cm^{-1} (CH_2, CH_3 bending) and 728 cm^{-1} (CH_2 bending), and peaks related to anhydride group were not observed. This is because the maleic anhydride grafting ratio in PE-g-MA was very low. In PE-g-MA/A-PA6, a 1724 cm^{-1} (C = O stretching) peak of maleic anhydride was identified and a chemical bond with A-PA6 could be expected.

From a result of PU, PU was confirmed to be thermoplastic polyether-based urethane. The urethane group was identified at 1698 cm^{-1}, 1659 cm^{-1} (free and hydrogen-bonded urethane

ULSAN NATIONAL INSTITUTE OF
SCIENCE AND TECHNOLOGY

C = O, stretching) peaks in PU. The corresponding peaks disappeared in PU/A-PA6, indicating the potential for occurrence of the reaction. In case of PA, all IR results of A-PA6, PA and PA/A-PA6 showed clear Amide I, II, III peaks, thus hydrogen bonding between amide groups of PA sizing material and A-PA6 matrix could be expected. From a result of EP, it was confirmed that sizing material EP is diglycidyl ether of bisphenol A (DGEBA) epoxy resin, and oxirane ring was identified by the peak 912 cm^{-1}. Comparing EP/A-PA6 composite with A-PA6 matrix, 1548 cm^{-1} peak disappeared. The peak at 1548 cm^{-1} is Amide II (in plane N-H bending vibration), which indicates the reaction occurred. As a result, the intensity of C=O stretching vibration was increased, resulting in Amide I peak shift to the higher wavenumber.

ULSAN NATIONAL INSTITUTE OF SCIENCE AND TECHNOLOGY

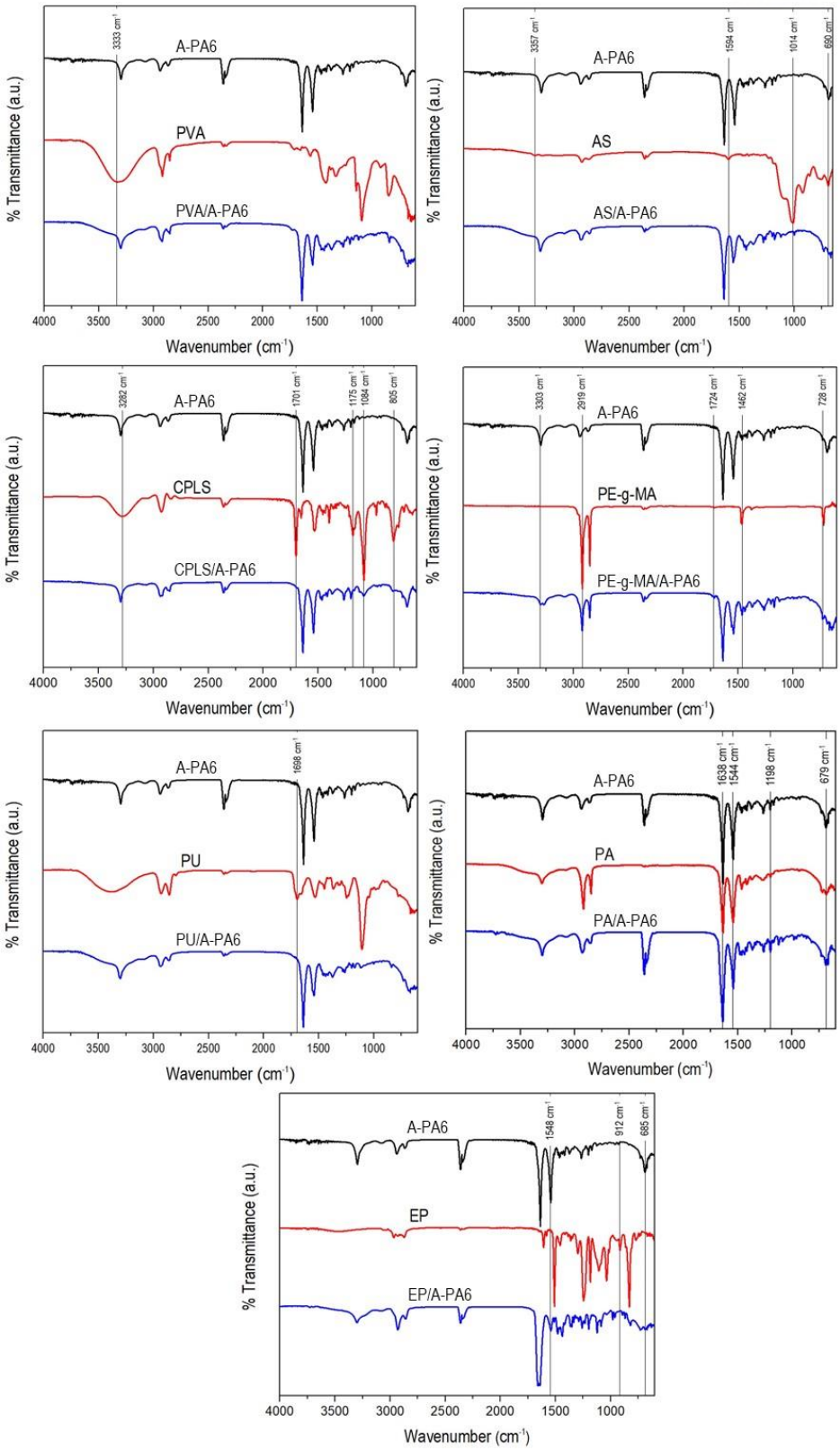

Figure 16. FT-IR spectra of A-PA6, sizing materials and sizing materials/A-PA6 polymer composites.

ULSAN NATIONAL INSTITUTE OF SCIENCE AND TECHNOLOGY

4.9. X-ray Micro CT Analysis

X-ray Micro CT analysis was performed to investigate the void content in the composite material depending on the sizing materials coated on the fiber surface, and the results are shown in the **Table 5**, and the results include only voids with a size larger than 9 μm. Except for CPLS, the same tendency with surface energy analysis was observed, especially EP and PA showed a much lower void content of 0.4 % than desized sample. As a result, it was confirmed that when the composite material is made of a resin having a high polar component ratio like A-PA6, it greatly affects the wettability. In contrast to the surface energy result, CPLS showed the highest void content result of 3.62%. During the sizing process, the caprolactam ring opened due to the presence of water and heat, forming a ε-aminocaproic acid (**Fig. 17**). The anion form of catalyst of A-PA6 matrix was deactivated by acidic carboxyl group on the surface of CPLS coated carbon fiber[39, 83]. As a result, CPLS interrupted anionic polymerization of PA6 and formed voids in the interface between fiber and matrix, which resulted in the highest void content for CPLS. This mechanism was successfully demonstrated by FT-IR and micro CT results. **Figure 18** shows void content results of EP-CF/A-PA6 and CPLS-CF/A-PA6 by 3D visualization.

Table 5. Void content of composite with different of sizing materials (> 9 μm).

Sizing materials	Desized	PVA	AS	CPLS	PE-g-MA	PU	PA	EP
Void content (%)	1.69	1.22	2.05	3.62	2.21	3.03	0.40	0.36

ULSAN NATIONAL INSTITUTE OF SCIENCE AND TECHNOLOGY

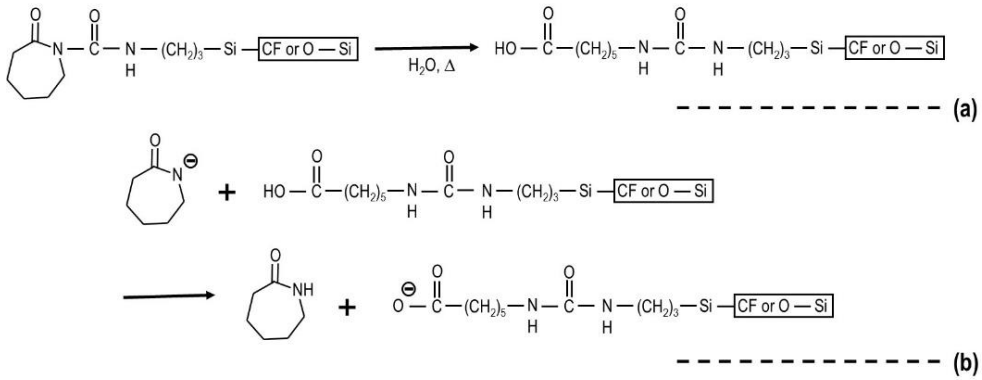

Figure 17. Reactions of CPLS and ε-caprolactam during polymerization: (a) production of ε-aminocaproic acid during sizing process and (b) deactivation of anions by acidic carboxyl groups of CPLS.

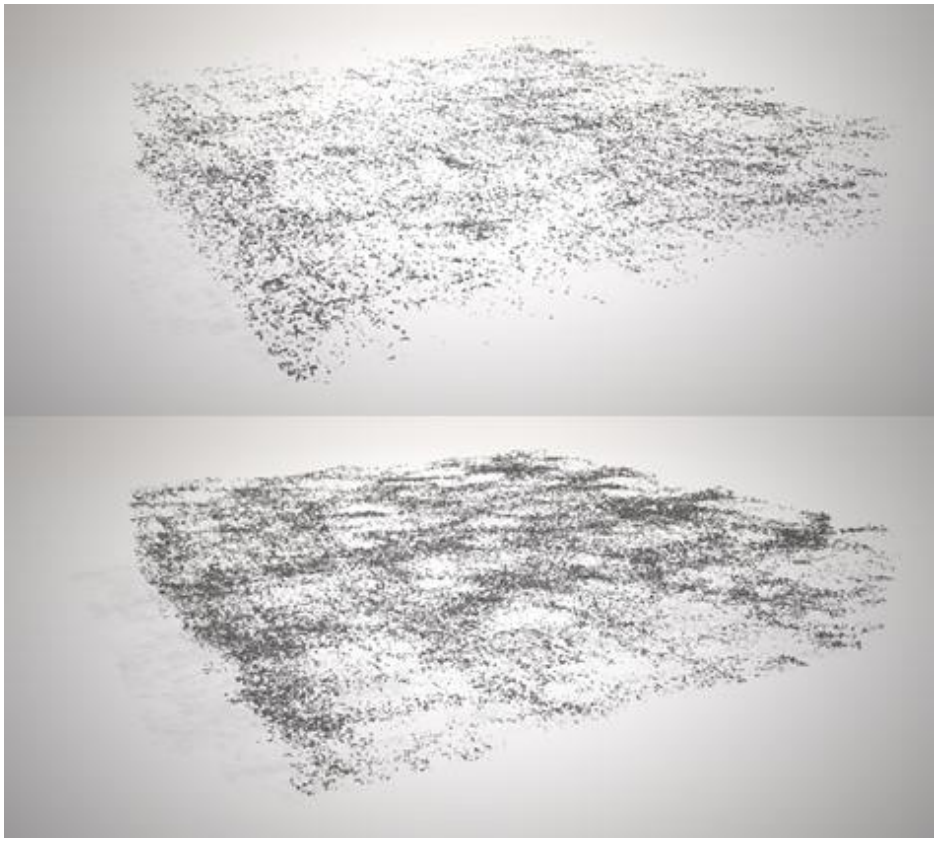

Figure 18. 3D visualization results of void content; EP-CF/A-PA6 (Top), CPLS-CF/A-PA6 (Bottom).

ULSAN NATIONAL INSTITUTE OF SCIENCE AND TECHNOLOGY

4.10. Fracture Surface Analysis

The fracture surfaces of the composite materials were identified by using SEM, and **Fig. 19** shows the fracture surfaces of EP-CF/A-PA6 and CPLS-CF/A-PA6. In case of the sample coated with EP, it was confirmed that the EP-coated carbon fiber and the A-PA6 resin were tightly bonded, and a large part of the resin was well-attached on the surface of the debonded fibers. It implies improved interphase and stronger interface of the EP-CF/A-PA6 composite. The CPLS coated sample, like the previous micro CT analysis, found a lot of voids at the interphase between the fiber and the resin, and the debonded fiber surface was very clean. That is, it showed poor interphase and weaker interface of the CPLS-CF/A-PA6.

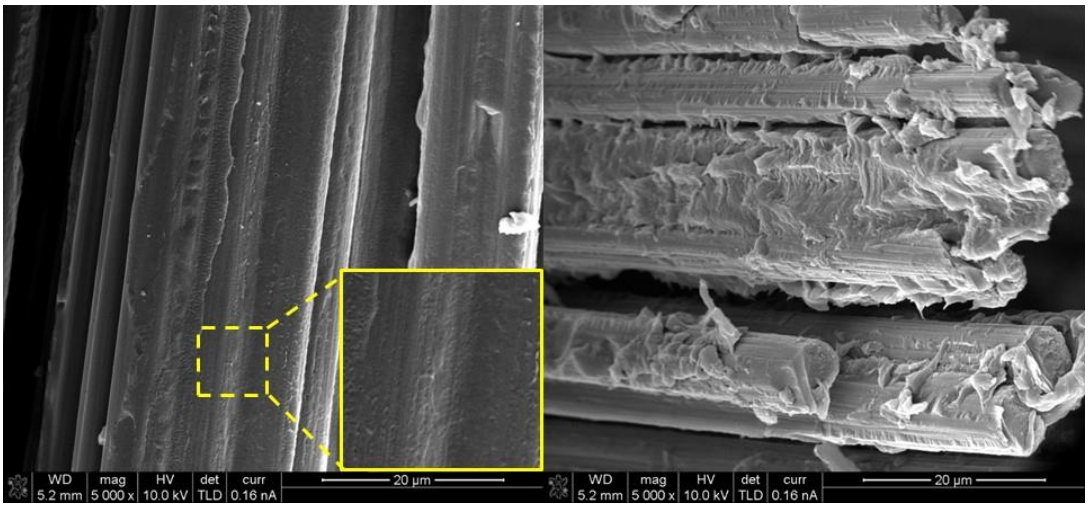

(a)

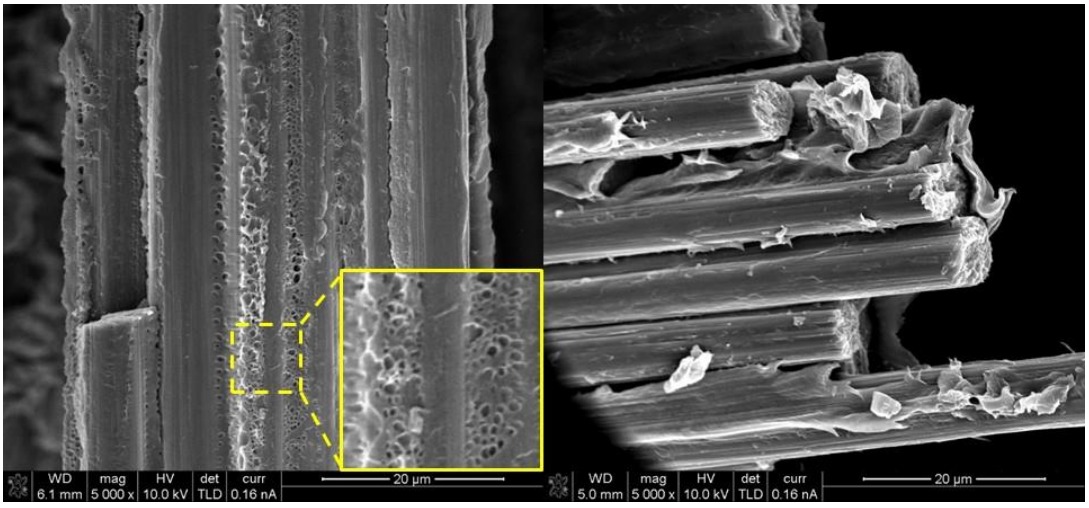

(b)

Figure 19. Fracture surfaces of (a) EP-CF/A-PA6, and (b) CPLS-CF/A-PA6.

ULSAN NATIONAL INSTITUTE OF SCIENCE AND TECHNOLOGY

5. Summary

The effects of sizing materials on the properties of carbon fiber-reinforced anionic polyamide 6 composites were investigated. First, desizing was performed by dipping commercial carbon fiber into acetone for 3 days and was confirmed by TGA. Next, 7 types of sizing materials were used to make sizing solutions. The sizing process was carried out by wetting the desized carbon fiber with the solution followed by heat treatment. 1-1.5 wt.% sizing content, which was determined to be the appropriate sizing level, was used for all the sizing processes. Subsequently, the sizing material-coated carbon fiber/A-PA6 composites were manufactured by using the T-RTM process.

TGA confirmed that all sizing materials were preserved during the T-RTM process. From XPS results, the changes of chemical compositions and functional groups on the fiber surface were investigated after the sizing process, and the activated carbon percent increased in EP-CF, PA-CF and PVA-CF samples. This can be expected to have a high chemical interaction with A-PA6 resin. Next, the surface energy of the fiber was analyzed. Both the total surface energy and the polar component ratio of PA-CF and EP-CF were higher than those of desized-CF. Both properties of CPLS-CF, PE-g-MA-CF and PU-CF samples decreased after sizing.

Fiber-bundle pull-out and short beam shear tests were performed using the composites manufactured by T-RTM, and IFSS and short beam strength were measured. Consequently, the highest improvements in IFSS and short beam strength were 30 and 50% achieved with EP and PA sizings, respectively, and both values of CPLS-CF/A-PA6 and PU-CF/A-PA6 decreased. The IFSS and short beam strength results showed similar tendencies, and especially the fluctuation in values of the short beam strength was larger than IFSS results, indicating that interlaminar interface strengthening effect of sizing material was expanded as the scale increases from a bundle to woven fibers.

To analyze the chemical interactions between the sizing materials and the A-PA6 resin, possible chemical reactions were investigated and confirmed by FT-IR analysis. Most sizing materials participated in the anionic ring opening polymerization of ε-caprolactam and formed a covalent bonding or a hydrogen bonding with A-PA6 resin.

X-ray micro CT analysis was performed to measure the void content inside the composite,

ULSAN NATIONAL INSTITUTE OF
SCIENCE AND TECHNOLOGY

showing the lowest void content in EP-CF/A-PA6 and PA-CF/A-PA6, and the highest void content in CPLS-CF/A-PA6 and PU-CF/A-PA6. This showed a trend consistent with the surface energy analysis. In particular, the acidic carboxyl group of CPLS deactivated the ion form of catalyst and interrupted anionic ring polymerization. This led to void formation in the interphase between fiber and matrix and weakened interface strength, and it was proven by the fracture surface analysis. **Figure 20** shows the improvement mechanisms of fiber-matrix adhesion in the case of EP-CF/A-PA6 and PA-CF/A-PA6.

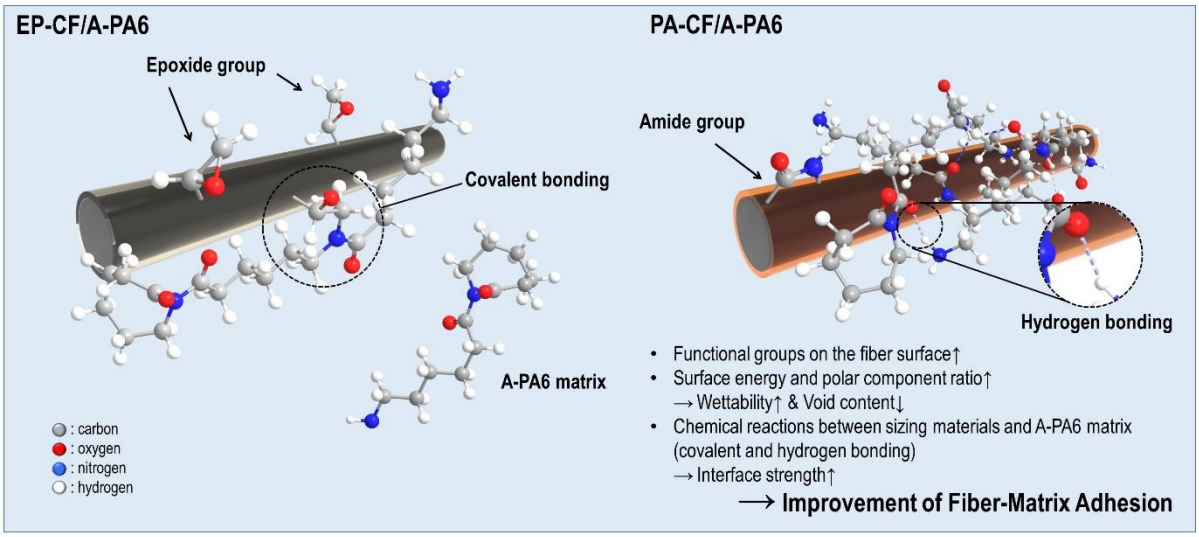

Figure 20. Improvement mechanisms of EP-CF/A-PA6 and PA-CF/A-PA6.

ULSAN NATIONAL INSTITUTE OF
SCIENCE AND TECHNOLOGY

6. Conclusions and Recommendation for Future Work

6.1. Conclusions

In order to investigate the effects of sizing materials on the properties of carbon fiber-reinforced anionic polyamide 6 composite, physical and chemical changes of the carbon fiber surface by the sizing materials were analyzed by TGA, SEM, XPS, FT-IR and X-ray micro CT. Also, fiber-bundle pull-out and short beam shear tests were conducted to measure the IFSS and short beam strength of the composite manufactured by T-RTM. The surface changes in the coated fibers affected the fiber-matrix adhesion in a complex way. The polar component ratio of surface energy and the activated carbon percent of the XPS analysis had a similar tendency, and it was also related to the void content of the composite. In addition, the chemical reactions between the sizing material and the resin improved interface strength of the composite, and conversely, decreased fiber-matrix adhesion due to the voids in the interphase induced by deactivation during the process. Therefore, various analysis results must be considered in selecting a sizing material suitable for the manufacturing process.

Consequently, the highest improvements in IFSS and short beam strength were 30 and 50% achieved with EP and PA sizings, respectively, due to enhanced fiber-matrix adhesion with A-PA6 resin. The improvement mechanisms of fiber-matrix adhesion by EP and PA were verified by XPS, surface energy, X-ray micro CT and FT-IR analysis. As a results, EP and PA sizing materials were proven to be the most suitable for T-RTM process.

6.2. Recommendations for Future Work

Based on the results of this study, we concluded the most suitable sizing materials for T-RTM process. However, the research was conducted under common conditions, optimizing the sizing process only for the sizing content of 1-1.5 wt.%. Adding a silane coupling agent to the EP and PA sizing solutions and optimizing the appropriate conditions will improve fiber-matrix adhesion better than this experiment was obtained.

In addition, CPLS was not suitable for the solution-dipping-based sizing process, resulting in reduced fiber-matrix adhesion. However, since the ε-caprolactam ring structure of CPLS is a monomer of A-PA6, it has a potential to be used in T-RTM process. Barfknecht *et al*.[53] has

ULSAN NATIONAL INSTITUTE OF SCIENCE AND TECHNOLOGY

studied single-stream processing technique by coating CPLS and initiator on glass fiber surfaces. As a result, the current injection of two solutions can be reduced to one. By combining the above studies, it can be expected that the fiber-matrix adhesion enhancement through the sizing, and simplification of the T-RTM process can be achieved simultaneously if the fiber surface is coated by CPLS and activator successfully without modification (**Fig. 21**). For the above research, it is necessary to perform a further study on the activator coating process, and the single-stream T-RTM process will be expected to have high potential with increasing demand for thermoplastic composite.

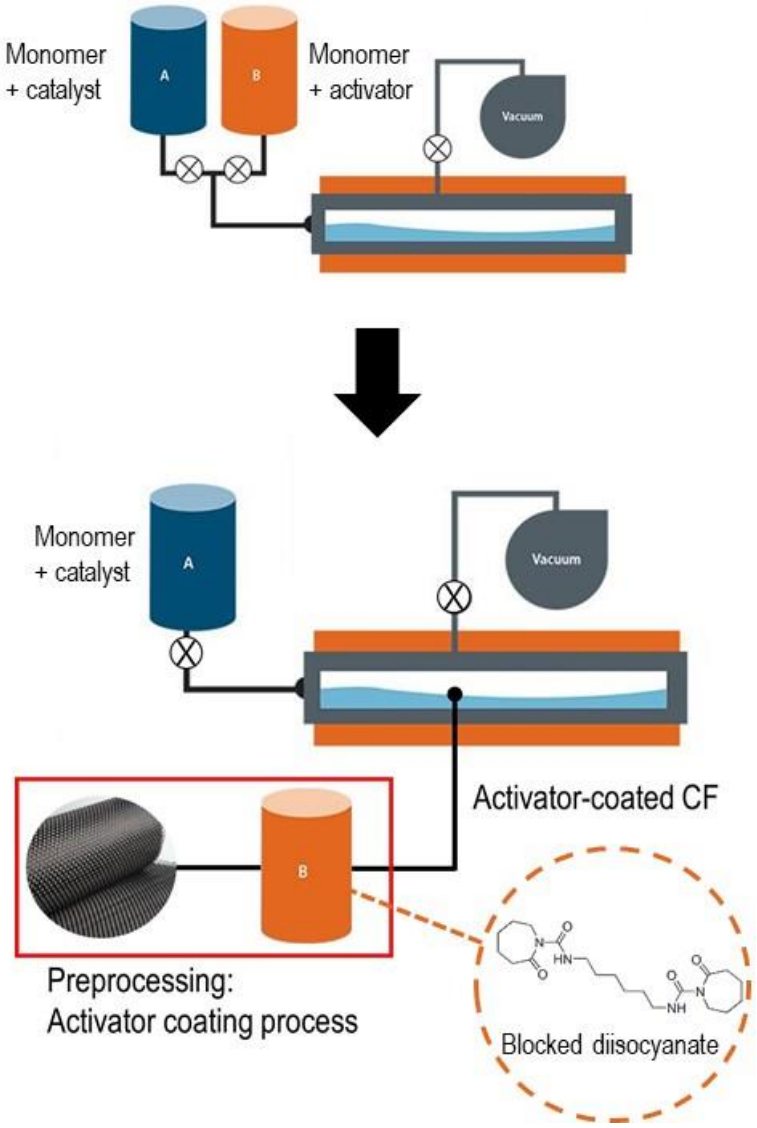

Figure 21. Schematic of single stream T-RTM process by preprocessing of activator coating.

ULSAN NATIONAL INSTITUTE OF SCIENCE AND TECHNOLOGY

References

1. van Rijswijk, K., Bersee, H. E. N., Reactive processing of textile fiber-reinforced thermoplastic composites - An overview, Compos Part a-Appl S 38(3) (2007) 666-681.
2. Berg, L. F., Process development for the reactive injection moulding of caprolactam intermediates, Fraunhofer-Verlag, 2011.
3. Pillay, S., Vaidya, U. K., Janowski, G. M., Liquid molding of carbon fabric-reinforced nylon matrix composite laminates, J Thermoplast Compos 18(6) (2005) 509-527.
4. Kim, B. J., Cha, S. H., Park, Y. B., Ultra-high-speed processing of nanomaterial-reinforced woven carbon fiber/polyamide 6 composites using reactive thermoplastic resin transfer molding, Compos Part B-Eng 143 (2018) 36-46.
5. Veedu, V. P., Cao, A. Y., Li, X. S., et al., Multifunctional composites using reinforced laminae with carbon-nanotube forests, Nat Mater 5(6) (2006) 457-462.
6. Kim, B. J., Cha, S. H., Kong, K., Ji, W., Park, H. W., Park, Y. B., Synergistic interfacial reinforcement of carbon fiber/polyamide 6 composites using carbon-nanotube-modified silane coating on ZnO-nanorod-grown carbon fiber, Compos Sci Technol 165 (2018) 362-372.
7. Gnadinger, F., Middendorf, P., Fox, B., Interfacial shear strength studies of experimental carbon fibers, novel thermosetting polyurethane and epoxy matrices and bespoke sizing agents, Compos Sci Technol 133 (2016) 104-110.
8. Allred, R. E., Wesson, S. P., Shin, E. E., et al., The influence of sizings on the durability of high-temperature polymer composites, High Performance Polymers 15(4) (2003) 395-419.
9. Dai, Z. S., Shi, F. H., Zhang, B. Y., Li, M., Zhang, Z. G., Effect of sizing on carbon fiber surface properties and fibers/epoxy interfacial adhesion, Appl Surf Sci 257(15) (2011) 6980-6985.
10. Visiongain, CFRP Composites Market Forecast 2014-2024, Visiongain, 2014.
11. Berger, R., Series production of high-strength composites, Roland Berger, 2012.
12. Sullivan, F., Strategic outlook of global electric vehicle market in 2014, Frost & Sullivan, 2014.
13. Lucintel, Status of the composites industry: market potentials and innovation mega trends, Lucintel, 2014.

ULSAN NATIONAL INSTITUTE OF SCIENCE AND TECHNOLOGY

14. Huntsman, "Dynamic fluid compression moulding(DFCM)," JEC Magazine No. 95, 2015.
15. Sharma, M., Gao, S. L., Mader, E., Sharma, H., Wei, L. Y., Bijwe, J., Carbon fiber surfaces and composite interphases, Compos Sci Technol 102 (2014) 35-50.
16. Vilatela, J. J., Eder, D., Nanocarbon Composites and Hybrids in Sustainability: A Review, Chemsuschem 5(3) (2012) 456-478.
17. Yu, K. J., Wang, M. L., Wu, J. Q., Qian, K., Sun, J., Lu, X. F., Modification of the Interfacial Interaction between Carbon Fiber and Epoxy with Carbon Hybrid Materials, Nanomaterials-Basel 6(5) (2016).
18. Pozegic, T. R., Anguita, J. V., Hamerton, I., et al., Multi-Functional Carbon Fiber Composites using Carbon Nanotubes as an Alternative to Polymer Sizing, Sci Rep-Uk 6 (2016).
19. Isitman, N. A., Aykol, M., Kaynak, C., Nanoclay assisted strengthening of the fiber/matrix interface in functionally filled polyamide 6 composites, Compos Struct 92(9) (2010) 2181-2186.
20. Thiagarajan, A., Palaniradja, K., Velmurugan, K., Effect of interfacial bonding on impact properties of chopped glass fiber polymer nanocomposites, Compos Interface 22(4) (2015) 265-280.
21. Shah, A. U. R., Prabhakar, M. N., Song, J. I., Current Advances in the Fire Retardancy of Natural Fiber and Bio-Based Composites - A Review, Int J Pr Eng Man-Gt 4(2) (2017) 247-262.
22. Pedrazzoli, D., Pegoretti, A., Expanded graphite nanoplatelets as coupling agents in glass fiber reinforced polypropylene composites, Compos Part a-Appl S 66 (2014) 25-34.
23. Jiang, S. A., Li, Q. F., Wang, J. W., He, Z. L., Zhao, Y. H., Kang, M. Q., Multiscale graphene oxide-carbon fiber reinforcements for advanced polyurethane composites, Compos Part a-Appl S 87 (2016) 1-9.
24. Pathak, A. K., Borah, M., Gupta, A., Yolcozeki, T., Dhakate, S. R., Improved mechanical properties of carbon fiber/graphene oxide-epoxy hybrid composites, Compos Sci Technol 135 (2016) 28-38.
25. Burn, D. T., Harper, L. T., Johnson, M., et al., The usability of recycled carbon fibers in

ULSAN NATIONAL INSTITUTE OF SCIENCE AND TECHNOLOGY

short fiber thermoplastics: interfacial properties, J Mater Sci 51(16) (2016) 7699-7715.

26. Borba, P. M., Tedesco, A., Lenz, D. M., Effect of Reinforcement Nanoparticles Addition on Mechanical Properties of SBS/Curaua Fiber Composites, Mater Res-Ibero-Am J 17(2) (2014) 412-419.
27. Dilsiz, N., Wightman, J. P., Surface analysis of unsized and sized carbon fibers, Carbon 37(7) (1999) 1105-1114.
28. Dilsiz, N., Wightman, J. P., Effect of acid-base properties of unsized and sized carbon fibers on fiber/epoxy matrix adhesion, Colloid Surface A 164(2-3) (2000) 325-336.
29. Liu, J. Y., Ge, H. Y., Chen, J., Wang, D. Z., Liu, H. S., The preparation of emulsion type sizing agent for carbon fiber and the properties of carbon fiber/vinyl ester resin composites, J Appl Polym Sci 124(1) (2012) 864-872.
30. Shim, J. W., Park, S. J., Ryu, S. K., Effect of modification with HNO3 and NaOH on metal adsorption by pitch-based activated carbon fibers, Carbon 39(11) (2001) 1635-1642.
31. Tiwari, S., Bijwe, J., Panier, S., Tribological studies on polyetherimide composites based on carbon fabric with optimized oxidation treatment, Wear 271(9-10) (2011) 2252-2260.
32. Feng, M. J., Wang, S. B., Yu, Y. L., Feng, Q. H., Yang, J. P., Zhang, B. M., The H3PO4/H2SO4/HNO3 Chemical Functionalization Optimized Performances of Functionalized Carbon Fibers via Preventing Fibers from Over-Oxidation, J Electrochem Soc 163(10) (2016) A2225-A2231.
33. Tiwari, S., Sharma, M., Panier, S., Mutel, B., Mitschang, P., Bijwe, J., Influence of cold remote nitrogen oxygen plasma treatment on carbon fabric and its composites with specialty polymers, J Mater Sci 46(4) (2011) 964-974.
34. Bismarck, A., Kumru, M. E., Springer, J., Influence of oxygen plasma treatment of PAN-based carbon fibers on their electrokinetic and wetting properties, J Colloid Interf Sci 210(1) (1999) 60-72.
35. Dong, J. D., Jia, C. Y., Wang, M. Q., et al., Improved mechanical properties of carbon fiber-reinforced epoxy composites by growing carbon black on carbon fiber surface, Compos Sci Technol 149 (2017) 75-80.
36. van Rijswijk, K., Bersee, H. E. N., Jager, W. F., Picken, S. J., Optimisation of anionic

ULSAN NATIONAL INSTITUTE OF SCIENCE AND TECHNOLOGY

polyamide-6 for vacuum infusion of thermoplastic composites: choice of activator and initiator, Compos Part a-Appl S 37(6) (2006) 949-956.

37. van Rijswijk, K., Bersee, H. E. N., Beukers, A., Picken, S. J., van Geenen, A. A., Optimisation of anionic polyamide-6 for vacuum infusion of thermoplastic composites: Influence of polymerisation temperature on matrix properties, Polym Test 25(3) (2006) 392-404.
38. van Rijswijk, K., Lindstedt, S., Vlasveld, D. P. N., Bersee, H. E. N., Beukers, A., Reactive processing of anionic polyamide-6 for application in fiber composites: A comparitive study with melt processed polyamides and nanocomposites, Polym Test 25(7) (2006) 873-887.
39. van Rijswijk, K., Teuwen, J. J. E., Bersee, H. E. N., Beukers, A., Textile fiber-reinforced anionic polyamide-6 composites. Part I: The vacuum infusion process, Compos Part a-Appl S 40(1) (2009) 1-10.
40. van Rijswijk, K., van Geenen, A. A., Bersee, H. E. N., Textile fiber-reinforced anionic polyamide-6 composites. Part II: Investigation on interfacial bond formation by short beam shear test, Compos Part a-Appl S 40(8) (2009) 1033-1043.
41. Pillay, S., Vaidya, U. K., Janowski, G. M., Effects of moisture and UV exposure on liquid molded carbon fabric reinforced nylon 6 composite laminates, Compos Sci Technol 69(6) (2009) 839-846.
42. Harper, L. T., Burn, D. T., Johnson, M. S., Warrior, N. A., Long discontinuous carbon fiber/polypropylene composites for high volume structural applications, J Compos Mater 52(9) (2018) 1155-1170.
43. Feng, M. J., Wang, S. B., Yu, Y. L., Feng, Q. H., Yang, J. P., Zhang, B. M., Carboxyl functionalized carbon fibers with preserved tensile strength and electrochemical performance used as anodes of structural lithium-ion batteries, Appl Surf Sci 392 (2017) 27-35.
44. Liu, J. Y., Ge, H. Y., Chen, J., Liu, H. S., Preparation of Epoxy Sizing Agent for Carbon Fiber by Phase Inversion Emulsification, Polym Polym Compos 20(1-2) (2012) 63-67.
45. Chen, J., Ge, H. Y., Liu, J. Y., Zhou, X. R., Wang, D. Z., Preparation of Waterborne Epoxy Resin for Carbon Fibers Sizing Agent, Asian J Chem 25(3) (2013) 1489-1491.
46. Dai, Z. S., Zhang, B. Y., Shi, F. H., Li, M., Zhang, Z. G., Gu, Y. Z., Chemical interaction

ULSAN NATIONAL INSTITUTE OF SCIENCE AND TECHNOLOGY

between carbon fibers and surface sizing, J Appl Polym Sci 124(3) (2012) 2127-2132.

47. Yao, L. R., Li, M., Wu, Q., et al., Comparison of sizing effect of T700 grade carbon fiber on interfacial properties of fiber/BMI and fiber/epoxy, Appl Surf Sci 263 (2012) 326-333.
48. Lee, G., Ko, K. D., Yu, Y. C., Lee, J., Yu, W. R., Youk, J. H., A facile method for preparing CNT-grafted carbon fibers and improved tensile strength of their composites, Compos Part a-Appl S 69 (2015) 132-138.
49. Kim, J., Mai, Y.-W., Effects of interfacial coating and temperature on the fracture behaviours of unidirectional Kevlar and carbon fiber reinforced epoxy resin composites, J Mater Sci 26(17) (1991) 4702-4720.
50. Cho, D.-H., Yun, S.-H., Kim, J.-K., et al., Effects of Fiber Surface-Treatment and Sizing on the Dynamic Mechanical and Interfacial Properties of Carbon/Nylon 6 Composites, Carbon letters 5(1) (2004) 1-5.
51. Jiang, S., Li, Q., Zhao, Y., Wang, J., Kang, M., Effect of surface silanization of carbon fiber on mechanical properties of carbon fiber reinforced polyurethane composites, Compos Sci Technol 110 (2015) 87-94.
52. Yuan, H., Wang, C., Zhang, S., Lin, X., Effect of surface modification on carbon fiber and its reinforced phenolic matrix composite, Appl Surf Sci 259 (2012) 288-293.
53. Barfknecht, P. W., Martin, J., Pillay, B., Vaidya, U. K., Gray, G. M., Single-stream processing technique for in situ polymerization of glass fiber/polyamide-6 laminates, J Thermoplast Compos 30(12) (2017) 1639-1653.
54. Herrera-Franco, P., Valadez-Gonzalez, A., A study of the mechanical properties of short natural-fiber reinforced composites, Composites Part B: Engineering 36(8) (2005) 597-608.
55. Gnädinger, F., Middendorf, P., Fox, B., Interfacial shear strength studies of experimental carbon fibers, novel thermosetting polyurethane and epoxy matrices and bespoke sizing agents, Compos Sci Technol 133 (2016) 104-110.
56. Unterweger, C., Bruggemann, O., Furst, C., Effects of different fibers on the properties of short-fiber-reinforced polypropylene composites, Compos Sci Technol 103 (2014) 49-55.
57. Pucci, M. F., Liotier, P.-J., Drapier, S., Capillary effects on flax fibers–Modification and

ULSAN NATIONAL INSTITUTE OF SCIENCE AND TECHNOLOGY

characterization of the wetting dynamics, Composites Part A: Applied Science and Manufacturing 77 (2015) 257-265.

58. Unterweger, C., Duchoslav, J., Stifter, D., Fürst, C., Characterization of carbon fiber surfaces and their impact on the mechanical properties of short carbon fiber reinforced polypropylene composites, Compos Sci Technol 108 (2015) 41-47.
59. Owens, D. K., Wendt, R., Estimation of the surface free energy of polymers, J Appl Polym Sci 13(8) (1969) 1741-1747.
60. Kaelble, D., Dispersion-polar surface tension properties of organic solids, The Journal of Adhesion 2(2) (1970) 66-81.
61. Zhou, J., Li, Y. G., Li, N. Y., Hao, X. Z., Liu, C. Q., Interfacial shear strength of microwave processed carbon fiber/epoxy composites characterized by an improved fiber-bundle pull-out test, Compos Sci Technol 133 (2016) 173-183.
62. Schell, J. S. U., Renggli, M., van Lenthe, G. H., Muller, R., Ermanni, P., Micro-computed tomography determination of glass fiber reinforced polymer meso-structure, Compos Sci Technol 66(13) (2006) 2016-2022.
63. Rudzinski, S., Häussler, L., Harnisch, C., Mäder, E., Heinrich, G., Glass fiber reinforced polyamide composites: Thermal behaviour of sizings, Composites Part A: Applied Science and Manufacturing 42(2) (2011) 157-164.
64. Dai, Z., Shi, F., Zhang, B., Li, M., Zhang, Z., Effect of sizing on carbon fiber surface properties and fibers/epoxy interfacial adhesion, Appl Surf Sci 257(15) (2011) 6980-6985.
65. Yao, L., Li, M., Wu, Q., et al., Comparison of sizing effect of T700 grade carbon fiber on interfacial properties of fiber/BMI and fiber/epoxy, Appl Surf Sci 263 (2012) 326-333.
66. Sarac, A. S., Tofail, S. A., Serantoni, M., Henry, J., Cunnane, V. J., McMonagle, J. B., Surface characterisation of electrografted random poly [carbazole-co-3-methylthiophene] copolymers on carbon fiber: XPS, AFM and Raman spectroscopy, Appl Surf Sci 222(1-4) (2004) 148-165.
67. Silva, R., Muniz, E. C., Rubira, A. F., Multiple hydrophilic polymer ultra-thin layers covalently anchored to polyethylene films, Polymer 49(19) (2008) 4066-4075.
68. Ma, J., Xu, Q., Gao, D., Zhou, J., Zhang, J., Blend composites of caprolactam-modified

ULSAN NATIONAL INSTITUTE OF SCIENCE AND TECHNOLOGY

casein and waterborne polyurethane for film-forming binder: Miscibility, morphology and properties, Polymer degradation and stability 97(8) (2012) 1545-1552.

69. Dilsiz, N., Wightman, J., Surface analysis of unsized and sized carbon fibers, Carbon 37(7) (1999) 1105-1114.
70. Song, W., Gu, A., Liang, G., Yuan, L., Effect of the surface roughness on interfacial properties of carbon fibers reinforced epoxy resin composites, Appl Surf Sci 257(9) (2011) 4069-4074.
71. Xie, J., Xin, D., Cao, H., et al., Improving carbon fiber adhesion to polyimide with atmospheric pressure plasma treatment, Surface and coatings technology 206(2-3) (2011) 191-201.
72. Luo, Y., Zhao, Y., Duan, Y., Du, S., Surface and wettability property analysis of CCF300 carbon fibers with different sizing or without sizing, Materials & Design 32(2) (2011) 941-946.
73. Zhang, R., Zhang, J., Zhao, L., Sun, Y., Sizing agent on the carbon fibers surface and interface properties of its composites, Fibers and Polymers 16(3) (2015) 657-663.
74. Yue, C., Padmanabhan, K., Interfacial studies on surface modified Kevlar fiber/epoxy matrix composites, Composites Part B: Engineering 30(2) (1999) 205-217.
75. Zhamu, A., Zhong, W., Stone, J., Experimental study on adhesion property of UHMWPE fiber/nano-epoxy by fiber bundle pull-out tests, Compos Sci Technol 66(15) (2006) 2736-2742.
76. Nuyken, O., Pask, S. D., Ring-opening polymerization—an introductory review, Polymers 5(2) (2013) 361-403.
77. Koulouri, E., Kallitsis, J., Miscibility behavior of Poly (vinyl alcohol)/Nylon 6 blends and their reactive blending with Poly (ethylene-co-ethyl acrylate), Polymer 39(11) (1998) 2373-2379.
78. Cui, L., Yeh, J. T., Wang, K., Fu, Q., Miscibility and isothermal crystallization behavior of polyamide 6/poly (vinyl alcohol) blend, Journal of Polymer Science Part B: Polymer Physics 46(13) (2008) 1360-1368.
79. Van Rijswijk, K., van Geenen, A., Bersee, H., Textile fiber-reinforced anionic polyamide-6 composites. Part II: Investigation on interfacial bond formation by short beam shear test, Composites Part A: Applied Science and Manufacturing 40(8) (2009)

ULSAN NATIONAL INSTITUTE OF SCIENCE AND TECHNOLOGY

1033-1043.

80. Fang, H., Yang, G., Influence of in situ compatibilization on in situ formation of low-density polyethylene/polyamide 6 blends by reactive extrusion, J Appl Polym Sci 116(5) (2010) 3027-3034.

81. Hou, L. L., Liu, H. Z., Yang, G. S., A novel approach to the preparation of thermoplastic polyurethane elastomer and polyamide 6 blends by in situ anionic ring-opening polymerization of ε-caprolactam, Polymer international 55(6) (2006) 643-649.

82. Gupta, A., Singhal, R., Nagpal, A., Crosslinking reaction of epoxy resin (diglycidyl ether of bisphenol A) by anionically polymerized polycaprolactam: I. Mechanism and optimization, J Appl Polym Sci 89(12) (2003) 3237-3247.

83. Zhang, X. C., Macdonald, D. A., Goosen, M. F. A., Mcauley, K. B., Mechanism of Lactide Polymerization in the Presence of Stannous Octoate - the Effect of Hydroxy and Carboxylic-Acid Substances, J Polym Sci Pol Chem 32(15) (1994) 2965-2970.

ULSAN NATIONAL INSTITUTE OF SCIENCE AND TECHNOLOGY

Acknowledgements

First of all, I would like to express my greatest gratitude to Professor Young-Bin Park for his personal and research support for my graduate course in the last 2 years. Thanks to his passionate guidance, I had a meaningful time learning a lot about the research. I was able to personally motivate and grow as I saw his sincere and passionate attitude. Also, I would like to thank Professor Wooseok Ji and Professor Han Gi Chae for their passionate consideration of my master's thesis. In addition, all the researchers who have been with Functional Intelligent Materials Lab (FIMLab), Dr. Byeong-Joo Kim, Beom-Gon Cho, Changyoon Jeong, Gu-Hyeok Kang, Hyung Doh Roh, Yoon-Bo Shim, Chan-Woo Joung, In-Yong Lee, Seong-Hwan Lee and Jeewon Heo, I would like to express my gratitude to all of you, especially, Dr. Kim and Shim for sincere assistance. Lastly, I thank my most precious family and girlfriend in my life.

I would like to thank UNIST for encouraging me to have a social and research experience from 2011 to 2018, and LG Display for supporting me to focus on the research.